



**Estimation Above Ground Biomass of Private Forest
Using Sentinel-1 and Sentinel-2 Satellite Data
(A Case Study in Gunung Kidul, Yogyakarta, Indonesia)**

Askar

**A Thesis Submitted in Fulfillment of the Requirements for the
Degree of Master of Science in Environmental Management
Prince of Songkla University
2018
Copyright of Prince of Songkla University**

Thesis Title Estimation Above Ground Biomass of Private Forest Using Sentinel-1 and Sentinel-2 Satellite Data (A Case Study in Gunung Kidul, Yogyakarta, Indonesia)

Author Mr. Askar

Major Program Environmental Management (International Program)

Major Advisor


.....
(Dr. Narissara Nuthammachot)

Co-advisor


.....
(Dr. Worradorn Phairuang)

Examining Committee:

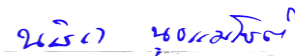

..... Chairperson
(Dr. Khamphe Phoungthong)



..... Committee
(Assoc. Prof. Dr. Kanchana Nakhapakorn)



..... Committee
(Dr. Akom Sowana)



..... Committee
(Dr. Narissara Nuthammachot)

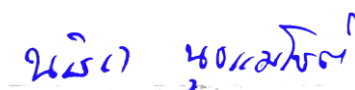


..... Committee
(Dr. Worradorn Phairuang)

The Graduate School, Prince of Songkla University, has approved this thesis as fulfillment of the requirements for the Master of Science Degree in Environmental management

.....
(Prof. Dr. Damrongsak Faroongsarng)
Dean of Graduate School

This is to certify that the work here submitted is the result of the candidate's own investigations. Due acknowledgement has been made of any assistance received.



.....Signature
(Dr. Narissara Nutahammachot)
Major Advisor



.....Signature
(Mr. Askar)
Candidate

I hereby certify that this work has not been accepted in substance for any degree, and is not being currently submitted in candidature for any degree.



.....Signature
(Mr. Askar)
Candidate

| | |
|----------------------|--|
| Thesis Title | Estimation Above Ground Biomass of Private Forest Using Sentinel-1 and Sentinel-2 Satellite Data (A Case Study in Gunung Kidul, Yogyakarta, Indonesia) |
| Author | Askar |
| Major Program | Environmental Management |
| Academic year | 2018 |

ABSTRACT

Private forest has crucial role in maintaining the functioning of Indonesian forest ecosystem especially the continuous degradation of natural forest. Private forest is a part of social forestry which becomes a tool for the Indonesian government to reduce Carbon dioxide (CO₂) emission by 26 % by 2030. The Reduction Emission Degradation and Deforestation (REDD) scheme has encouraged the Indonesian government to establish forest monitoring system by estimating forest carbon stock using a combination of forest inventory and remote sensing. This study aimed to assess potential Sentinel-1 and Sentinel-2 for estimating Above Ground Biomass (AGB) of private forest. We found that gamma VH delivered from sentinel-1 had significant correlation with AGB whereas parameters from sentinel-2 which had significant correlation with AGB were B3, B4, NDI45, NDVI, SR, IRECI, EVI and NDI75. Combination between NDI45 and EVI through Stepwise linear regression fitted for establishing model between field AGB and vegetation indices ($R^2 = 0.81$). We also found that the AGB in the study area based on spatial analysis was 72.54 ton/ha. A Root Mean Square Error (RMSE) value from predicted and observed AGB was 27 ton/ha. AGB in private forest is categorized into moderate class due to behavior of the farmers to cut the forest in particular time. Overall, vegetation indices more superior than spectral value and radar backscatter to assess AGB in private forest.

Keywords : Above ground biomass ; Private forest ; Sentinel-1 ; Sentinel-2

ACKNOWLEDGMENT

I would like to express sincere gratitude to my major advisor, Dr. Narissara Nuthammachot, for his guidance, encouragement, and support during my research. I would like to express special gratitude to Dr. Worradorn Phairuang, for his valuable advice and guidance, to finish this study.

I would like to thank you to the chairperson of the thesis examination Dr. Khampee Phoungthong and member of committee Assoc. Prof. Dr. Kanchana Nakhapakorn, Dr Akom Sowana, Dr Narissara Nuthammachot and Dr. Worradorn Phairuang for their valuable comments and recommendations for my thesis. I would like to deliver special thanks to the external examiner of my thesis, for the suggestion.

I would like to express my thanks to staff of Environmental Management for their patience and accuracy. I would like to thank to Girisekar and Jetis group of farmers for allowing me to conduct data collection for this reserach.

I would like to thank to Graduate School, Prince of Songkla University for the financial support during my master program through Thailand's Education Hub for Southern Region of ASEAN Countries (TEH-AC) scholarship. This research was supported by PSU Graduate School Research Support Funding for Thesis.

Finally, my greatest thank is to my beloved family for their support and caring to encourage me to finish my study. Their strong love gave me strength to finish my study.

Askar

TABLE OF CONTENTS

| | |
|--|------------|
| ABSTRACT | v |
| ACKNOWLEDGMENT..... | vi |
| TABLE OF CONTENTS..... | vii |
| LIST OF TABLES..... | ix |
| LIST OF FIGURES..... | x |
| LIST OF EQUATIONS..... | xi |
| LIST OF ABBREVIATIONS..... | xii |
| CHAPTER 1. INTRODUCTION..... | 1 |
| 1.1. Background..... | 1 |
| 1.2. objectives..... | 4 |
| 1.3. Research questions..... | 5 |
| 1.4. Outcomes..... | 5 |
| 1.5. Significance of study..... | 5 |
| CHAPTER 2. LITERATURE REVIEW..... | 6 |
| 2.1. Private forest..... | 6 |
| 2.2. Biomass..... | 7 |
| 2.3. Radar image..... | 8 |
| 2.4. Optical image..... | 11 |
| CHAPTER 3. MATERIALS AND METHODS..... | 15 |
| 3.1. Study area..... | 15 |
| 3.2. Materials..... | 16 |
| 3.3. Field data..... | 18 |
| 3.4. Pre-Processing satellite image..... | 21 |
| 3.5. Classification process..... | 25 |
| 3.6. Retrieval of backscatter,spectral and vegetation indices value..... | 25 |
| 3.7. Statistical analysis..... | 26 |
| 3.8. Creating AGB map..... | 28 |

| | |
|---|-----------|
| 3.9. AGB map validation..... | 28 |
| CHAPTER 4. RESULT AND DISCUSSION | 30 |
| 4.1. Descriptive analysis of field data..... | 30 |
| 4.2. Private forest map..... | 31 |
| 4.3. Correlationship between AGB and Sentinel-1 data..... | 32 |
| 4.4. Correlationship between AGB and Sentinel-2 spectral reflectance..... | 35 |
| 4.5. Correlationship between AGB and Sentinel-2 vegetation indices..... | 37 |
| 4.6. Modeling AGB in private forest..... | 39 |
| 4.7. AGB map validation..... | 40 |
| 4.8. Mapping AGB in private forest..... | 42 |
| CHAPTER 5. CONCLUSION..... | 45 |
| REFERENCES..... | 47 |
| APPENDIX..... | 53 |
| VITAE..... | 68 |

LIST OF TABLES

| | |
|--|----|
| Table 1. Resume of some research about carbon sequestration in indonesia | 6 |
| Table 2. Description of Sentinel-1 SAR..... | 10 |
| Table 3. Sentinel-2 bands..... | 13 |
| Table 4. Comparison the number of private and state forests in Gunung Kidul..... | 15 |
| Table 5. Software used during research..... | 17 |
| Table 6. List of field equipment used in this study..... | 17 |
| Table 7. Detailed specification of Sentinel-1A data used in this study..... | 18 |
| Table 8. Detailed specification of Sentinel-2A data used in this study..... | 18 |
| Table 9. Allometric equations used to estimate AGB..... | 20 |
| Table 10. A List of vegetation indices..... | 22 |
| Table 11. Important value index for each species in this study area..... | 30 |
| Table 12. Correlation and linear regression between backscatter and AGB..... | 33 |
| Table 13. Correlation and linear regression between spectral reflectance and AGB..... | 35 |
| Table 14. Correlation and linear regression between vegetation indices and AGB..... | 37 |
| Table 15. Summary of paramaters for AGB model development..... | 40 |
| Table 16. Summary of AGB estimating in private forest..... | 43 |

LIST OF FIGURES

| | |
|---|----|
| Figure 1. Total emission emitted by each sector..... | 2 |
| Figure 2. The study area..... | 16 |
| Figure 3. Map of sample plots disribution..... | 19 |
| Figure 4. A desain of sample plot for data collection..... | 20 |
| Figure 5. Speckle filtering image..... | 23 |
| Figure 6. Retrieval pixel value from NDVI..... | 26 |
| Figure 7. Flowchart of the study | 29 |
| Figure 8. Distribution of field AGB within the sample plot..... | 31 |
| Figure 9. Private forest map unit derived from supervised classification..... | 31 |
| Figure 10. Scatter plot between AGB and VH backscatter..... | 33 |
| Figure 11. Scatter plot between AGB and VV backscatter..... | 34 |
| Figure 12. Scatter plot between AGB and spectral reflectance..... | 36 |
| Figure 13. Scatter plot between AGB and vegetation indices..... | 38 |
| Figure 14. Scatter plot of observe and predicted AGB..... | 41 |
| Figure 15. AGB map of the study area..... | 42 |

LIST OF EQUATIONS

| | |
|---|----|
| Equation 1. Allometric equation of teak | 20 |
| Equation 2. Allometric equation of silk..... | 20 |
| Equation 3. Allometric equation of mahagoni..... | 20 |
| Equation 4. Allometric equation of akasia..... | 20 |
| Equation 5. Allometric equation of others tree..... | 20 |
| Equation 6. Radiometric calibration..... | 23 |
| Equation 7. Radiometric terrain flattening | 24 |
| Equation 8. Linear regression..... | 27 |
| Equation 9. Multilinear regression..... | 27 |
| Equation 10. Root mean square error | 28 |
| Equation 11. AGB model in this study..... | 40 |
| Equation 12. Linear model of AGBvalidation..... | 41 |

LIST OF ABBREVIATIONS

| | |
|-----------------|--|
| AGB | Above Ground Biomass |
| ATCOR | Atmospheric and Topographic Correction |
| BEF | Biomass Expansion Factor |
| BOA | Bottom of Atmosphere |
| CCC | Canophy Chlorophyl Content |
| CCRS | Canadian Centre of Remote Sensing |
| CIFOR | Centre for International Agroforestry Research |
| COP | Confrence of Party |
| CO ₂ | Carbondioxide |
| DBH | Diameter at Breats Height |
| DEM | Digital Elevation Model |
| DRTC | Doppler Range Terrain Correction |
| ESA | European Space Agency |
| EVI | Enhance Vegetation Index |
| FWI | Forest Watch Indonesia |
| GCP | Ground Control Points |
| GEMI | Global Environmental Vegetation Index |
| GPS | Global Positioning System |
| HH | Horizontal Horizontal |
| HV | Horizontal Vertical |
| IRECI | Inverted Red Edge Vegetation Index |
| IVI | Important Value Index |
| IWI | Interferometric Wide Mode |
| LAI | Leaf Area Index |
| LULULF | Land Use, Land Use Change and Forestry |

| | |
|-------|--|
| MOEF | Ministry of Environmental and Forestry of Indonesia |
| MSAVI | Modified Soil Vegetation Index |
| MCARI | Modified Chlorophyll Absorption in Reflectance Index |
| NDI45 | Normalised Difference Index 45 |
| NDI75 | Normalised Difference Index 75 |
| NDVI | Normalised Difference Vegetation Index |
| NIR | Nearinfrared |
| REDD | Reduction Emission Degradation and Deforestation |
| REIP | Red Edge Position Index |
| RF | Relative Frequency |
| RD | Relative Density |
| RD1 | Relative Dominant |
| RMSE | Root Mean Square Error |
| SNAP | Sentinel Application Form |
| SAR | Synthetic Aperture Radar |
| SAVI | Soil Adjustment Vegetation Index |
| SR | Simple Ratio |
| SRTM | Shuttle Radar Topography Mission |
| S2REP | Sentinel-2 Red Edge Position index |
| TOA | Top of Atmosphere |
| VH | Vertical Horizontal |
| VV | Vertical Vertical |
| UTM | Universal Transverse Mercator |

CHAPTER 1

INTRODUCTION

1.1. Background

Deforestation is a major problem for countries that have a large number of tropical rain forests like Brazil, Congo and Indonesia. Deforestation is the long-term permanent loss of forest cover through the conversion of forest into another land cover type [1]. Deforestation in Indonesia has been increasing rapidly and has become a global concern. Recently, as a report by Margono et al. (2014) about Indonesia deforestation showed that Indonesia lost natural forest over 6.02 million hectares during 2000 – 2012 and the number of deforestation increased around 46,000 hectares annually [2]. Margono et al. (2014) added that the higher rate of deforestation in Indonesia occurred in 2012, accounted for 0.84 million ha. It overshadowed the deforestation rate in Brazil which reached 0.46 million ha in the same year [2]. Hansen et al. (2009) used multi-temporal data from MODIS and AVHRR satellite images to evaluate the deforestation rate in Indonesia during 1990 – 2005 [3]. The study reported that the rate of deforestation in Indonesia between 1990 – 2000 was 1.79 million ha/year, whereas in 2000 – 2005 the rate was 0.71 million ha/year [3]. There were many factors that contributed to the phenomenon. In 2009, Forest Watch Indonesia (FWI) exposed that palm oil plantations, timber concessions, pulp and paper industries and forest fires were the major factors of Indonesian deforestation [4].

Deforestation has not only driven Indonesia to lose the forest areas but also has increased greenhouse gas emission. World Bank (2007) revealed that 75% of greenhouse gas emission in Indonesia was contributed by the forestry sector [5]. Based on statistical data from Ministry of Environment and Forestry of Indonesia (MOEF), the average rate of greenhouse gases in Indonesia during 2000 - 2013 was as much as 1.262 Gt (CO₂), dominated by the forestry sector (LULUCF) [6] (Figure 1).

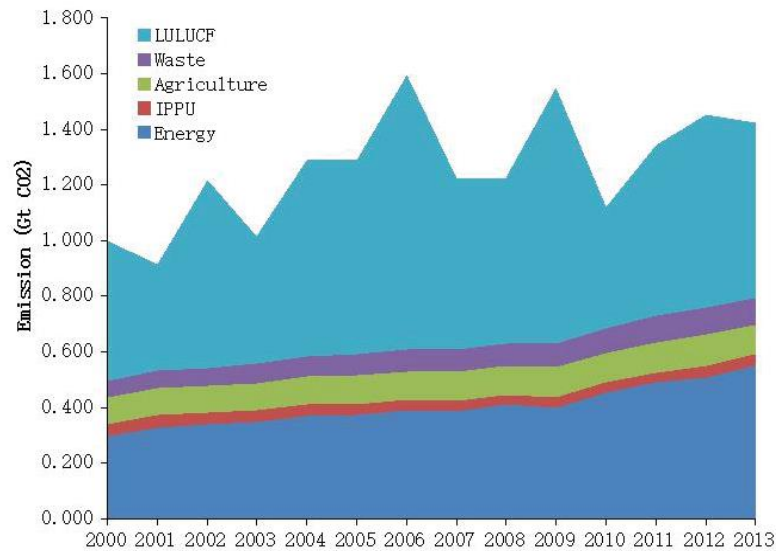


Figure 1. Total emission emitted by each sector

Indonesian government has intended to reduce greenhouse gas emission. It is proved by the commitment of this country at the 21st of Conference of Parties (COP) to reduce global greenhouse gas emission at 26% by 2030 [7]. Social forestry then is one of the programs to achieve the goal. Through the program, the government attempts to conserve ecosystem and landscape [7]. In Indonesia, social forestry has long been conducted in private lands and forest areas (state forest). Particularly in the forest areas, Indonesian government has prepared 12.7 million ha or 10% of the number of Indonesian forest during 2015 – 2019 to be distributed to the farmers [8]. It was known that Ministry of Environment and Forestry has distributed 192,031 ha of forest areas to the farmers by the middle of 2016 [9].

The second type of social forestry in Indonesia is a private forest. The main difference between private forest and natural forest in Indonesia is vegetation. It can be said that in the natural forest, vegetation will grow naturally, managed legally by the government and distributed over a large area [10]. In contrast, in the private forest, vegetation will be cultivated by farmers on their land and owned by themselves [10]. Policy brief released by Center for International Forestry Research (CIFOR) (2015) showed that the number of the private forests in Indonesia were around 2.8 million ha

[11]. The establishment of social forestry both in private lands and forest areas will not only improve the livelihood of the farmers but also will increase carbon sequestration, forest biomass and reduce greenhouse gas emission.

The 16th COP held in Mexico in 2010 resulted in a concept of Reduction Emission Degradation and Forest Deforestation (REDD) + as a recognition of efforts to reduce green house gasses emission outside the natural forests [12]. REDD + activities include forest deforestation and degradation, the mission of conservation, sustainable forests and improvement of forest carbon sink [12]. The concept of REDD + will not only be applicable in the forest areas but also in the private lands as long as they can increase carbon sink and reduce carbon dioxide (CO₂) [12]. The concept allows the farmers to include the private forests in Indonesia to access funding from the others countries or organizations which concern on global warming. Therefore, information of carbon and biomass in the private forest is very important as data base to deal with REDD + that will be implemented in 2020. For implementing REDD +, each member of United Nations Frame Work Convention of Climate Change (UNFCCC) including Indonesia has to establish forest monitoring system [13]. The methodology recommended is a combination of remote sensing and ground-based forest carbon inventory [13].

Remote sensing has been widely used for estimating Above Ground Biomass (AGB). Several studies reported the advantages of optical image utilization such as SPOT [14], Landsat [15] [16], and Terra Aster [17] for estimating AGB. To estimate AGB, determining correlation between spectral value or vegetation index and measured AGB from ground data collection in the sample plots is commonly applied. However, there is a major problem to procure optical images, which mainly come from cloud cover particularly in tropical areas such as Brazil, Indonesia and Malaysia. Therefore, to overcome that issue, radar satellite images were used since it can penetrate clouds and provide image with free clouds cover. A number of researchers have reported the use of radar satellite image for estimating AGB [17] [18] [19] with different kinds of radar satellite images, for example ALOS-PALSAR [20], RADARSAT [18], ENVISAT ASAR [21] and ERS-2 [17]. Currently, researchers have examined combination between optical and radar images to obtain AGB information [22] [14].

Several attempts have been made to know AGB of forestry sector using high resolution of satellite images [23]. Along with the progress, there are still obstacles. For instance, Foody et al. (2003) stated that AGB model which has been established in a region cannot be applied in other areas despite having close vegetation, thereby, it is imperative to develop a new model of AGB estimation [24]. Moreover, although the application of high resolution can increase accuracy of land cover mapping, it is costly particularly in large areas [25]. These problems become more serious in developing countries and institutions or researchers with low budget. Thus, the application of free or low cost satellite image for AGB estimation is important [25].

Sentinel-1 and Sentinel-2 Satellite data are new satellite images provided by ESA European Space Agency (ESA). Sentinel-1 is Synthetic Aperture Radar (SAR), providing C band with centre frequency of 5.405 GHz and it was launched in 2014. Sentinel-2 is an optical image with 13 spectral bands: 4 bands at 10 m, 6 bands at 20 m and 3 bands at 60 m spatial resolution and it was released in 2015. Both satellites can be freely downloaded from ESA website (<https://scihub.copernicus.eu/dhus>). Sentinel-1 and Sentinel-2 can be applied for mapping and monitoring the forest areas and measuring biophysical structure of the vegetation like AGB and growing stock volume. However, there is lack evidence about AGB investigation especially for utilization of Sentinel-1 and Sentinel-2 for predicting AGB on the private forest in Indonesia.

1.2. Objectives

The major objectives of this research are following:

1. To develop model for estimating AGB on private forest based on parameters from Sentinel-1 data, Sentinel-2 data and AGB data from the field.
2. To assess Sentinel-1 and Sentinel-2 remote sensing data in order to improve the estimation accuracy of private forest AGB.
3. To examine the potential of satellite data for AGB mapping on private forest.

1.3. Research questions

This study aimed to address the following questions:

1. What is the correlation between Sentinel-1 parameters (VV/VH backscatter values), Sentinel-2 parameters (spectral values and vegetation indices) and AGB measurement of private forest from sample plots?
2. What is the contribution of combination between Sentinel-1 parameters and Sentinel-2 parameters to establish AGB on private forest through multilinear regression?
3. How much distribution of AGB of private forest which is stored on the study area?

1.4. Outcomes

The outcome of this research is AGB model from integration between AGB measurement of private forest from sample plots and the satellite image parameters. Another outcome is the AGB map of private forest in study area based on selected model.

1.5. Significance of study

The study provides an important opportunity to advance the understanding of Sentinel-1 and Sentinel-2 image usage. Both Sentinel-2 and Landsat 8 can capture large areas, but Sentinel-2 has a better temporal and spatial resolution than Landsat 8 images. Sentinel-1 is a useful option where clouds are persistent because SAR data is not weather dependent.

CHAPTER 2

LITERATURE REVIEW

2.1. Private forest

Based on the Indonesia Forestry Regulation No. 41/1999, a private forest is forest developed in a private land [26]. The complete definition of private forest can be seen on a decision letter of Indonesian Forestry Minister No. 49/Kpts-II/1997 which explains that a private forest grows in a private land, has a minimum area of 0.25 hectares and minimum canopy closure of 50% [27]. Private forest can be divided by three categories which are full private forest, mix private forest, and agroforestry [28]. Full private forest is cultivated by a kind of tree, mix private forest is cultivated by more than one tree and agroforestry is mixed between trees and agriculture commodity [28].

Private forest has a significant role in reducing greenhouse gas emission in Indonesia because it can absorb CO₂ from the air and convert it to biomass. Carbon value can be inferred 50% from dry biomass [29]. The table below shows the resume of some research on carbon sequestration on private forests in Indonesia [30]:

Tabel 1. Resume of some researches about carbon sequestration in Indonesia

| No | Location | Carbon | Source |
|----|--|---|------------------|
| 1 | Private forest in Dengok Village, Gunung Kidul Regency | 49 ton/Ha | Aminuddin (1998) |
| 2 | Private forest in Karya Sari Village, Bogor Regency | 15.56 - 194.97 ton/ha | Asyisanti (2004) |
| 3 | <i>Albazia falcataria</i> private forest | Class of diameter 5 - 10 (0.0 ton/ha) 10 - 15 (0.99 ton/ha) 15 - 20 (1.75 ton/ha) 20 - 25 (6.42 ton/ha) 25 - 30 (5.24 ton/ha) 30 - 40 (8.26 ton/ha) 40 - 50 (20.306 ton/ha) 50 - Up (34.378 ton/ha) | Rachman (2009) |

Source : Centre of Research and Development of Policy and Climate Change, Ministry of environmental and forestry of Indonesia

2.2. Biomass

Biomass is described as the living organic matters that is present above ground and it expresses the mass of material per unit area. In general, carbon in forests can be grouped into five types based on the position on the ground [31]. They are above ground biomass (AGB) (stems, soil, branches, barks and side), below ground biomass (roots), dead wood, litter and soil organic carbon [31]. In regard to measurement methods, direct measurement of below ground biomass is hard to do since it requires root collection [32]. So, most studies on biomass measurement have focused on AGB as it is more simple in data collection and it accounts the majority of the AGB widely [33] [25] [34].

There are two ways to estimate AGB from the [31] [35]. The first is the field measurement method (biomass expansion factor and allometric equation) and the second is remote sensing [31]. Developing Biomass Expansion Factor (BEF) and allometric equation requires tree sample element such as branches, leaves, stems and twigs through the harvesting method [36] [37]. The fresh weight and oven – dried weight of these component then are measured. BEF converts volume (m³/ha) from terrestrial inventory to the biomass value [29]. Allometric equation will generates relationship between component of tree (diameter or height) and biomass from tree harvesting. Basuki et al. (2009) established allometric equation for lowland dipterocarp forest in Borneo Indonesia [38]. They sampled 122 trees and developed allometric equations by establishing relationship between AGB with diameter at breast height, commercial bole height and wood density [38]. Navar J. (2009) harvested 873 trees to develop allometric equations for temperate forest and tropical dry forest in Mexico [39]. Then, he estimated AGB based on the selected equations and resulted AGB around 130 Mg/Ha in temperate forest and 73 Mg/ha in tropical dry forest [39]. In forest areas, several studies argued that allometric equation would show a good performance in area where it was naturally established and could result in some errors if it was applied in outside [33]. Nelson et al. (2008) found that there was AGB overestimated when they estimated AGB in tropical forest in Amazonia brazil using some published tropical forest allometric equations [40]. Field measurement method is

more accurate to estimate biomass since it can access biomass directly but data collection is time consuming, expensive and is hampered by geographic and inaccessible area [25] [15].

Secondly, remote sensing method using radar and optical images is applied to estimate AGB from ecosystem. To predict biomass, model is established through correlation between biomass measurement derived sample plot and parameters from the image based on pixel value. Remote sensing has the ability to capture large and difficult areas which is the limitation of the field measurement method [15] [35]. In the past three decades, a number of researchers have sought to determine AGB from forest areas with different vegetation. Pedro et al. (2015) used RADARSAT-2 to estimate AGB on regenerating mangrove forest in Brazil [18]. The study showed that sigma nought (σ^0) value has better correlation than beta nought (β^0) and gamma nought (γ^0) to develop AGB in the mangrove forest [18]. In a study which utilize vegetation indices from Landsat 5, Wani et al.(2014) found that AGB value of conifer forest in Himalayan India is 0 – 400 ton/ha. In 2014, Hamdan et al. (2014) published a paper in which described utilisation of ALOS PALSAR to estimate AGB of tropical forest in Trengganu Malaysia [20]. The study showed that HV polarization more capable to estimate AGB in the tropical forest than HH Polarization [20]. Eckert (2012) used WorldView-2 to estimate AGB at Tropical forest in Madagascar [23]. The study of Eckert demonstrated application of image texture and vegetation indices as parameters for estimating AGB [23].

2.3. Radar image

Radar is acronym of radio detection and ranging which use radio waves for detecting an object, determining their distance and their angular position [41]. Radiation of radar signals can penetrate through cloud cover, all weather conditions and record surface of the world at any time, day or night. Signal from the sensor of radar is transmitted to the object then backscatter from the object will be processed by the sensor to create image. The volume of backscatter depends on roughness and the angle of the objects when signals are transmitted from the sensor [42]. Lilesand et al. (2008) highlighted backscatter as fraction energy that is reflected back to the sensor as result of interaction between signals from the sensor and the object [41]. Signal power,

directly or log transformed in decibel unit is used to represent the value of backscatter [41].

Radar emits pulse and receives backscatter from the side perpendicular to the direction of flight, that is called side looking radar [41]. Distortion of radar image appears because radar measures object through slant range than horizontal distance on the ground and various of topography and valley when the sensor interact with the object [42]. It will result varying scale of the image and the object does not represent actual size and distance. To tackle that issue, terrain correction should be applied on radar pre-processing before further analysis. Based on Canadian Centre of Remote Sensing (CCRS) (2014), there are three forms of radar image distortion: shadow, foreshortening, and layover [42]. Synthetic Aperture Radar, or often called SAR is one of remote sensing systems using microwave for recognizing objects. The system utilizes a short physical antenna because the sensor is less able to carry a long physical antenna. To overcome the size limitation, the forward motion of the sensor and data recording modification are used to simulate a very long antenna and produce finer azimuth resolution [41] [42].

Radar images have been used widely for estimating AGB in many types of radar images such as RADARSAT[18], ALOS PALSAR [22], DLR – ESAR [20], ENVISAT ASAR [21]. Gashemi et al. (2010) mentioned that type of bands and polarization are important to assess AGB in forest areas [22]. SAR data are commonly extracted in X, C, L, and P bands and each band has different characteristics in regard to vegetation structure. Backscatter from X band comes from leaves and surface layer of trees. Whereas, source of C band backscatter comes from leaves and small branches. Trunk and main branches are the main sources of L band backscatter. P and L band wavelength are longer than the X and C band so it can penetrate deeply through canopy cover and get backscatter from trunk [19]. P and L band are more capable to estimate AGB from the forest areas than X and C band [15] [19] [43]. Polarisation is orientation of electric field on electromagnetic waves, resulting from interaction between signals that have been transferred by sensor and reflector [19]. The types of polarisation are HH (signals transmitted and backscattered in horizontal), HV (signals transmitted on horizontal and backscattered on vertical), VV (signals transmitted and backscattered on vertical) and VH (signals transmitted on vertical and backscattered on horizontal) [19] [42].

Sentinel-1A Synthetic Aperture Radar (SAR) data is generated by the Sentinel-1 satellite recording belong to Europe which was launched in 3 April 2014 [44]. In April 2016, ESA launched Sentinel-1B which has similar characteristic with Sentinel-1A [45]. Both satellites carry a SAR sensor to record the earth's surface using C-band at frequency of 5.405 Hz. The satellite image can operate well in cloud area, rain condition, day or night so the result of the recording is free from weather distortion and clouds. Summary of Sentinel-1 SAR is provided in the table below [44] [45]:

Table 2. Description of Sentinel-1 SAR

| No | Aspects | Description |
|----|-------------------------------------|---|
| 1 | Launched | Sentinel-1A : April 2014, Sentinel-1B : April 2016 |
| 2 | Mission | <ul style="list-style-type: none"> • Land monitoring of forest, water, soil and agriculture • Marine monitoring • Sea observation • Mapping oil spill |
| 3 | Mission orbit | 6 days |
| 4 | C band instrument | Centre frequency : 5.405- 6 Ghz Incident angle : 20 – 45 Polarization : VV/VH,HH /HV,HH,VV |
| 5 | Mode, swatch widths, and resolution | <ul style="list-style-type: none"> • Strip map mode : 80 Km, 5 m x 5 m spatial resolution • IW swath : 250 km, 5 x 20 m resolution • Wave mode : 20 m x 20 m, 5 x 5 spatial resolution |
| 6 | Product | L-0 Raw, L-1 SLC, L-1 GRD, L-2 Ocean |

Source : Sentinel 1 Hand book

Although Sentinel-1 is relatively new, this image has been used for many purposes especially for land monitoring. For example, Abdikan et al. (2016) demonstrated the ability of Sentinel-1 to classify land cover in Istanbul Turkey [46]. Furthermore, Bayanuddin et al. (2016) investigated AGB in forest community in Sukoharjo Indonesia using Sentinel-1 [47]. The result showed low correlation between AGB and VV/VH value [47]. Former study revealed that C band had less ability to

predict AGB from dense vegetation than L and P bands because L and P bands can penetrate deep through canopy and get backscatter from the trunk [43]. C band will saturate in biomass level around 60 - 70 Mg/Ha compared to L band that can capture AGB value around 160 Mg/Ha [43].

To improve the level of C band for predicting AGB in the forest areas, there are some innovations have been done by the scientists. Castillo et al. (2016) added elevation as a parameter beside backscatter value from Sentinel-1 SAR to estimate AGB on the mangrove forest in Honda Bay beach Philippines [48]. Another way to improve estimation AGB is by combining SAR data and optical image data [22] [14]. For instance, Huang et al. (2016) combined backscatter value from ENVISAT ASAR and vegetation indices of Landsat image to calculate AGB in Xixi national wetland park in China [17].

2.4. Optical image

Optical satellite image systems use energy from the sun to recognize objects on surface. It is usually called passive sensor which can only be used to detect objects when the energy from the sun is available through earth illumination process. So, the sensor could not work at the night because no energy available. Energy from the sun is absorbed or reflected in visible wavelength and more reflected or reemitted on the infrared wavelengths [42].

Each object on the surface of the earth has different spectral responses to the electromagnetic energy from the sun. The colour of the water looks blue because high reflectance of energy electromagnetic in blue wavelength and became dark on near infrared because high absorbing of energy electromagnetic [39]. In near infrared and green wavelength, vegetation will be bright and green to the people's eye especially in summer. Chlorophyll on the leaves absorbs radiation more in blue and red wavelength and reflects green wavelength [42]. In the other hand, healthy leaves reflect more energy on near infrared wavelength [42]. Absorption will decrease when the autumn season since the number of chlorophylls is less. Consequently, reflectance of red will higher than near infrared and green and the color of healthy vegetation will be red or yellow [42]. Crops which has low near infrared and green reflectance and high red reflectance can be identified as stress crops.

Remote sensing using vegetation indices has been widely used for predicting AGB. Vegetation indices are image conversion of two or more bands that is created to improve the contribution of vegetation structure [49]. Determining of vegetation indices can be using mathematical function and each index has different formula. The most common index that have been widely used for measuring biophysics of vegetation is Normalization Difference Vegetation Index (NDVI). NDVI is calculated from ratio between difference and sum of near infrared reflectance and red reflectance [50]. The NDVI value for dense vegetation is around 0.4 – 0.8, shrub and meadow between 0.2 – 0.3 and cloud less than 0. However, NDVI value is sensitive to soil brightness particularly in areas with less vegetation cover and it is also influenced by the effect of atmosphere from aerosol. In fact, Huete et al. (2002) found that signature from canopy background like water, dead wood, falling leaves can influence the value of NDVI [49]. To overcome that problems, there are some vegetation indices have been established by the scientists. For example, Soil Adjustment Vegetation Index (SAVI), Modified Soil Adjustment Vegetation Index (MSAVI), and Modified Soil Adjustment Vegetation Index2 (MSAVI2) are established to reduce the effect of the soil response in low vegetation cover [51]. Enhancement Vegetation Index (EVI), furthermore, is useful to reduce the effect of the canopy background, to increase saturation level on dense vegetation and to decrease effect of aerosol [49] and Global Environmental Vegetation Index (GEMI) is created to minimalize the effect of the atmosphere [52].

Regarding its utilization, vegetation indices have been widely used for AGB estimation with different satellite images. In 2016, Hamdan et al. used SPOT 5 to assess AGB in the forest area in Trengganu Malaysia with various vegetation indices [14]. Similarly, Devagiri et al. (2013) investigated AGB for different types of vegetation in Karnataka India using NDVI from MODIS satellite image [53]. Gaspari et al. (2010) used NDVI for predicting AGB in the tropical dry forest of Argentina ($R^2 = 0.610$) with biomass range from sample plot 54 – 136 ton/ha using Landsat 7 ETM [54]. Vitchanakorn et al. (2014) used combination between various vegetation indices and spectral reflectance to assess AGB in Savannaket Lao PDR [25]. Optical image has problems in dense vegetation because of data saturation. Landsat image will saturate in the forest area with range 100 – 150 ton/ha in the moist tropical forest [15].

Sentinel-2A launched at 23 June 2015 in French Guiana and it is part of Copernicus European Space Agency (ESA) program. Sentinel-2 offers data which has similarity to Landsat 8 and SPOT and it can be used in agricultural and forestry monitoring, disaster assessment risk mapping. The Sentinel-2 image has swath width of 290 km, repeating the cycles earth in 5 days and has 13 bands with 3 resolutions (10 meter, 20 meter and 60 meter) [44]. The table below provides Sentinel-2 bands, their range and their resolution [56] :

Table 3. Sentinel-2 bands

| No | Band | Band range (nm) | Band center (nm) | Resolution (m) |
|----|--------------------------|-----------------|------------------|----------------|
| 1 | B1- Coastal Aerosol | 433 – 453 | 443 | 60 |
| 2 | B2 – Blue | 458 – 523 | 490 | 10 |
| 3 | B3 – Green | 543 – 578 | 560 | 10 |
| 4 | B4 – Red | 650 – 680 | 665 | 10 |
| 5 | B5 - Vegetation Red Edge | 698 – 713 | 705 | 20 |
| 6 | B6 - Vegetation Red Edge | 734 – 748 | 740 | 20 |
| 7 | B7 - Vegetation Red Edge | 765 – 785 | 783 | 20 |
| 8 | B8 – NIR | 785 – 900 | 842 | 10 |
| 9 | B8a -Vegetation Red Edge | 855 – 875 | 865 | 20 |
| 10 | B9 - Water Pavour | 930 – 950 | 945 | 60 |
| 11 | B10 - SWIR/Cirrus | 1365 – 1385 | 1375 | 60 |
| 12 | B11 – SWIR | 1565 – 1655 | 1610 | 20 |
| 13 | B12 – SWIR | 2100 – 2280 | 2190 | 20 |

Source : <https://eox.at/2015/12/understanding-sentinel-2-satellite-data>

Based on Sentinel-2 user hand book (2015), the product of sentinel-2 image are [55]:

1. **Level 0** and level **1 – A** which are not released to users.

2. Level 1–B

The Level-1B product is the lowest product level made available to users. It has been applied by radiometric correction which includes dark signal correction pixel response non- uniform, crosstalk, defective pixels, restoration and binning 60 meter bands.

3. Level 1-C

Level 1–C can be downloaded directly from the ESA website (<https://scihub.copernicus.eu/dhus>). The product is available on geometric and radiometric corrected in Top of Atmosphere (TOA).

4. Level 2-A

Output of the Level 2-A is Bottom of Atmosphere (BOA) corrected atmosphere product. BOA represents surface reflectance from conversion of TOA reflectance of level 1-C product.

Level 2-A is not readily available since it needs pre-processing (atmospheric correction) from level 1-C product through sen2cor Plugin in Sentinel Application Platform (SNAP) software. SNAP is designed by ESA to process Sentinel-1 and Sentinel-2. Pre-processing in Sen2cor plugin in SNAP requires large of memory so the computer has to be equipped with at least 8 GB of RAM.

One of differences between Sentinel-2 image and Landsat 8 OLI is the availability of red edge bands in Sentinel-2, that is usually called narrow band. The position of red edge bands (5,6,7) is between red and NIR band where chlorophyll strongly absorbs in red and strongly reflectance from leave cell structure in NIR. The main purpose of band 5 (705 nm), band 6 (740 nm), and band 7 (783 nm) is to improve monitoring vegetation [57]. The red edge bands cover the portion of the spectrum where reflectance significantly improve from the red region to the NIR region [58].

Sentinel-2 image provides vegetation indices like the other optical images (NDVI, EVI, SAVI, GEMI and others). There are some new vegetation indices coming from band combination of Sentinel-2, especially red edge bands. The vegetation indices coming from Sentinel-2 image are Inverted Red Edge Vegetation Indices (IRECI), Normalization Difference Index from band 4 and 5 (NDI 45), Sentinel-2 Red Edge Position Index (S2REP), Red edge Inflection Point Index (REIP) and Modified Chlorophyll Absorption in Reflectance Index (MCARI) [59][60]. In an investigation into chlorophyll assessment using Sentinel-2 simulation, Delgado et al. (2011) reported that NDI 45 can improve accuracy of chlorophyll estimation [61]. Castillo et al. (2016) used Sentinel-2 to estimate AGB of mangrove Forest in Honda Bay Beach Philippines [48]. The study showed that IRECI and NDI 45 more capable than NDVI to estimate AGB in mangrove forest [48].

CHAPTER 3

MATERIALS AND METHODS

3.1. Study area

Geographically, the study area is situated in 8° 01' 15" N and 110° 27' 30" E (Fig.2). The area is located in Jetis and Girisekar private forest management unit in Gunung Kidul Region, Yogyakarta Province, Indonesia. Girisekar is one of the 19 private forest management units that have been certified by TUV Rheinland. The study area covers an area of approximately 2,650 Ha (26.5 Km²). The annual mean temperature is 27° C with maximum temperature of 32.4 ° C and minimum temperature of 23.2 ° C [62]. The climate type is warm with annual rainfall of 1,602 mm/year [62]. The rainy season is mainly from october to may. The area is occupied by limestone mountain with elevation of 250 – 300 meter [62].

The private forest in Gunung Kidul regency in Yogyakarta province is one of large private forests and has become a model of private forest management in Indonesia. The number of forest community in Gunung Kidul are provided by the Table 4 below [63] :

Tabel 4. Comparison the number of private and state forest in Gunung Kidul

| No | Year | Forest area (Ha) | |
|----|------|------------------|--------------|
| | | Private forest | State forest |
| 1 | 2006 | 28,630 | 14,896 |
| 2 | 2010 | 31,672 | 14,896 |
| 3 | 2013 | 41,954 | 14,896 |

Source : <http://bappeda.jogjaprov.go.id/>

Table 4 shows that the number of the private forests in Gunung Kidul are higher than that of the state forests. It means that the private forests have a significant impact in reducing greenhouse gas emission in Yogyakarta and, therefore, the private forest is a source of AGB accumulation.

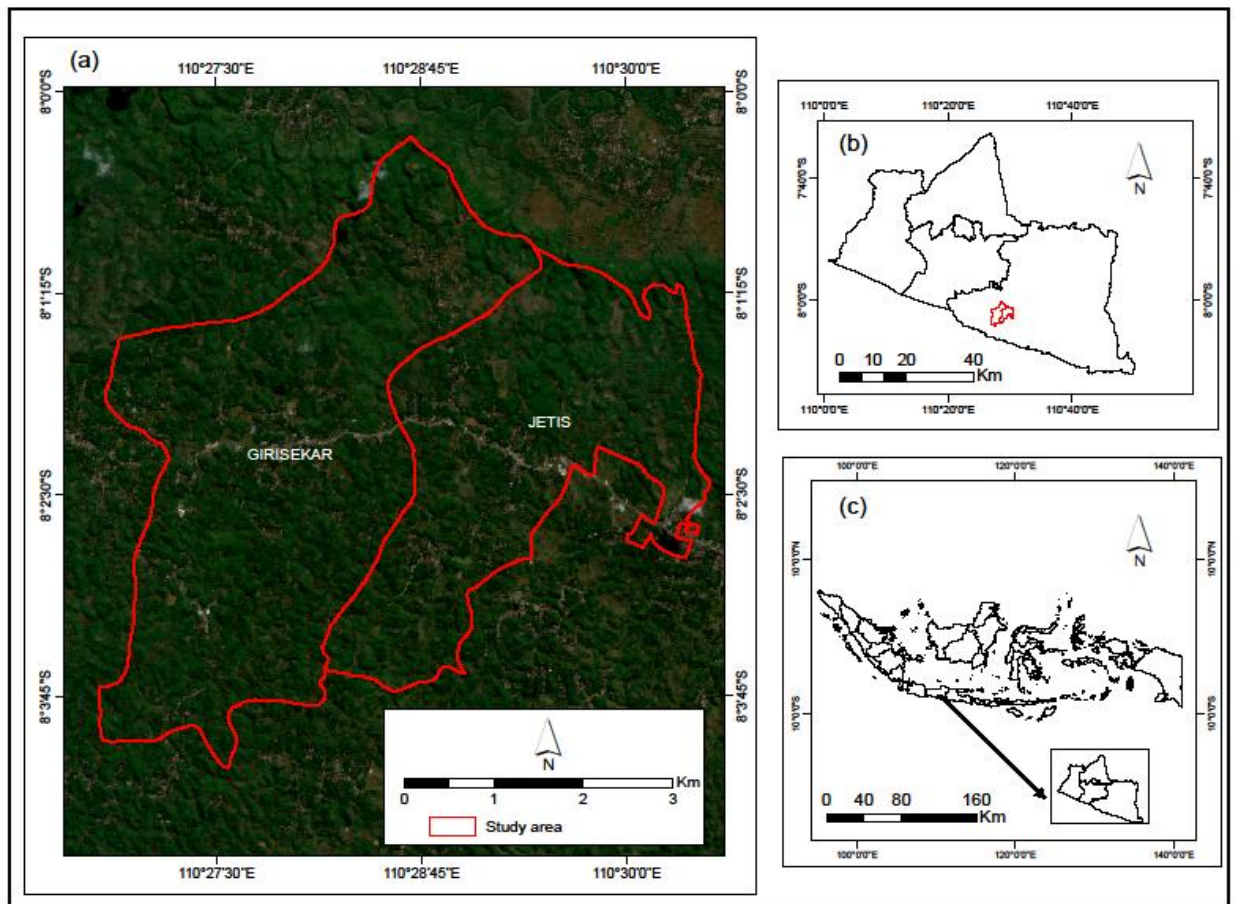


Figure 2. The study area (a) map of Girisekar and Jetis (b) The location of study area in Yogyakarta Province, (c) The location of Yogyakarta Province in the Indonesian map

3.2. Materials

Materials utilised for this study consisted of softwares, field equipments and satellite data. Therefore, this section explains the list of materials used in order to carry out this research.

3.2.1 Software

Several software were used during research. One of them is Sentinel Application Platform (SNAP). SNAP is open source software released by ESA to support pre-processing of Sentinel-1 and Sentinel-2. A list of software used in this study is shown by Table 5 below:

Table 5. Software used during research

| No | Software | Usage |
|----|-----------------|---|
| 1 | SNAP | <ul style="list-style-type: none"> ➤ Pre processing Sentinel -1 ➤ Pre processing Sentinel- 2 |
| 2 | ArcMap 10.5 | <ul style="list-style-type: none"> ➤ Subsetting of study area from the whole image ➤ Retrieving radar backscatters, spectral values and vegetaton indices values ➤ Producing AGB map ➤ Lay outing AGB map |
| 3 | SPSS 17 | <ul style="list-style-type: none"> ➤ Correlation analysis ➤ Regression analysis ➤ Validation model |
| 4 | Envi classic | <ul style="list-style-type: none"> ➤ Land cover classification ➤ Image accuracy assesement |
| 5 | Microsoft excel | <ul style="list-style-type: none"> ➤ Creating scatter plot ➤ Retrieving AGB field from field data ➤ Preliminary study of AGB model |

3.2.2 Field equipments

Field equipments were used to collect data. Table 6 summarised numerous equipments used in this study.

Table 6. Lists of field equipments used in this study

| No | Equipment | Use |
|----|---------------------|-----------------------------|
| 1 | Diameter tape | Measuring diameter of trees |
| 2 | Sunto clinometer | Measuring height of trees |
| 3 | GPS | Marking of sample plots |
| 4 | Distance meter tape | Measuring radius of plots |
| 5 | Field sheets | Recording field data |

3.2.3. Remote sensing data

Details of satellite image that will be used on this research are shown in Table 7:

Table 7. Detailed specification of Sentinel-1A data used in this study

| | | |
|----|--------------------|--|
| 1 | Mission | Sentinel-1A |
| 2 | Sensor type | Radar-C band |
| 3 | Radar Type | Level 1 GRDH (Ground Range Detected High Resolution) |
| 4 | Acquisition mode | IW (Interferometric Wide Mode) |
| 5 | Orbit Circle | 109 |
| 6 | Orbit Track | 127 |
| 7 | Polarization | VV/VH |
| 8 | Range resolution | 10 meter |
| 9 | Azimuth resolution | 10 meter |
| 10 | Time Recording | 19 May 2017 |
| 11 | Pass | Ascending |
| 12 | Detail of product | S1A_IW_GRDH_1SDV_20170519T105745_20170519T105814_016649_01BA24_42B9.SAFE |

Source : Sentinel-1A metadata

Table 8. Detailed specification of Sentinel-2A data used in this study

| | | |
|---|--------------------|---|
| 1 | Mission | Sentinel-2A level 1-C |
| 2 | Product type | S2MSI1C |
| 3 | Orbit Number | 89 |
| 4 | Spectral bands | 13 |
| 5 | Spatial Resolution | 10 meter : Band 2,3,4 and 8 20 meter : Band 5,6,7,8A,11 and 12 60 meter : Band 1,9 and 10 |
| 6 | Time Recording | 19 May 2017 |
| 7 | Pass | Descending |
| 8 | Details of product | S2A_MSIL1C_20170519T023351_N0205_R089_T49MDN_20170519T025549.SAFE |

Source : Sentinel-2A metadata

3.3. Field data

3.3.1. Field sampling design

Field data was collected in September 2017 and the end of November 2017. A total of 45 plots were set up. We used 30 plots for establishing model and another 15 plots for model validation. A stratified random sampling method was applied to select the plots based on accessibility, size and type of trees. This sampling method was used to ascertain areas with low and high AGB in community forest that would be sampled. Since data collection in forest area was limited by time, budget and geographical

condition, many researchers collected data based on their ability with normally 10 – 50 plots [14] [17] [18] [20] [22] [47] [53]. Utilization of 35 sample plots for modelling is based on the minimum sample that is required for statistical analysis.

3.3.2. Field data collection

As many as 45 plots established using the random sampling method were subjected to field data collection (Figure 3). We used a rectangle plot for collecting data. The size of the actual plot on the field would be 20 x 20 m as to pixel size of Sentinel-1 and Sentinel-2. The radius of the plot was 10 m from the edge of imaginary line (Figure 4). Therefore, the center of plot would be connective point. Coordinate of the center point then was recorded by GPS.

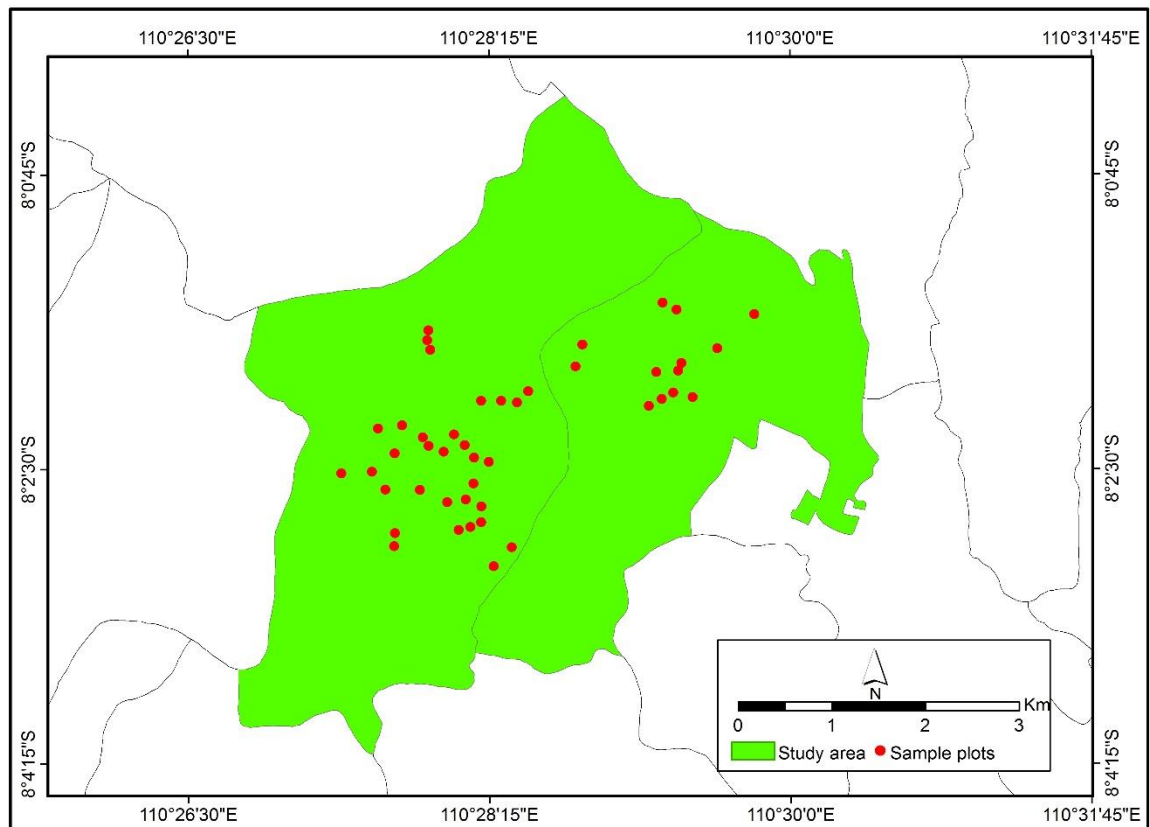


Figure 3. Map of sample plots distribution

All trees within the sample plots were measured. The main parameters recorded during the fieldwork were circumference (1.3 m above the ground) and height of trees. Moreover, the additional data measured was elevation on the selected plots. Circumference of trees was measured using tape meter and height was measured by sunto clinometer.

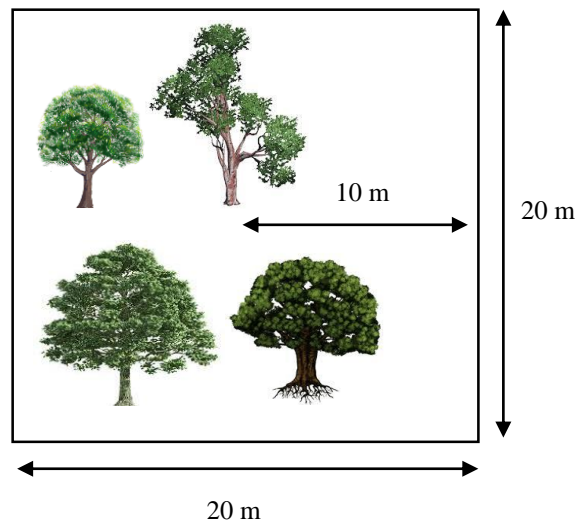


Figure 4. A design of sample plot for data collection

3.3.3. Field data analysis

Field data processing was conducted to calculate AGB based on data collected from the sample plots. AGB calculation was derived from allometric equations expressed by formula below [64]:

Table 9. Allometric equations used to estimate AGB

| No | Species | Allometric equation |
|----|---|------------------------------------|
| 1 | Teak (<i>Tectona grandis</i>) | $AGB = 0.0149 (D^2H)^{1.0835}$ (1) |
| 2 | Silk (<i>Paraserianthes falcataria</i>) | $AGB = 0.0199 (D^2H)^{0.9296}$ (2) |
| 3 | Mahagoni (<i>Swietenia mahagony</i>) | $AGB = 0.9029 (D^2H)^{0.684}$ (3) |
| 4 | Akasia (<i>Acacia auricaliformis</i>) | $AGB = 0.0775 (D^2H)^{0.9018}$ (4) |
| 5 | Other trees | $AGB = 0.0219 (D^2H)^{1.012}$ (5) |

D = Diameter at breast height at 1.3 meter above the ground (cm), H = Height (m) AGB = Above ground biomass (Kg/tree)

3.4. Pre-processing satellite images

3.4.1. Pre-processing Sentinel-2 Image

3.4.1.1. Atmospheric and Topographic Correction (ATCOR) Sen2cor

A Sentinel-2 image was downloaded from copernicus scientific data hub website. It has been scaled to TOA level including orthorectification and spatial registration on a global reference system [55]. Sentinel-2 Level 1-C was processed to Level 2-A to gain BOA corrected reflectance image using ATCOR Algorithm through Sen2cor plugin in SNAP. Output of this process was an orthoimage of surface reflectance in sentinel level-2A product and ready for further analysis [55]. Spectral value from band 3,4,5,6,7 and 8 were used as predictor for AGB estimation of private forest.

3.4.1.2. Resample image

Resample was a process to change pixels or spatial resolution of satellite images. This process is important to process satellite images with different resolution. Sentinel-2 has vegetation indices which combine band 3,4,5,6,7 and 8 where the location of the bands are in 10 and 20 meter resolution. Therefore, it is necessary to equalize spatial resolution so that bands can be used together in the analysis. To minimalise effect of geolocation error, each image was resampled to 20 m resolution than 10 m using a nearest neighbor method. The nearest neighbor method was used during the process since this method utilized spectral values and vegetation indices which are established from original Sentinel-2 band. This method does not alter the original value of the new image because it fills pixel value from the corrected image with the value of the nearest pixel from the original method [42].

3.4.1.3. Vegetation indices calculation

Vegetation indices were directly determined after atmospheric correction and resample. Calculation of vegetation indices was conducted by using band math module in SNAP software. Vegetation indices images were presented in Bean dimap (Snap) and Geotiff format. For this study, we used two vegetation indices called Sentinel-2 vegetation indices and traditional vegetation indices. Traditional indices involve NDVI, EVI, SR whereas Sentinel -2 vegetation indices include Normalization Difference Index from Band 5 and 6 (NDI 75), NDI 45 and IRECI. Traditional indices were selected based on simplicity and robustness. SR and NDVI work through simple

algorithm which employ ratio of NIR and RED bands. EVI is the robust index and has sensitivity to high biomass regions due to correction factor useful to eliminate influence of aerosol and canopy background [49]. Details of the indices used as predictor for biomass estimation is described by Table 10 below:

Table 10. A list of vegetation indices

| No | Vegetation indices | Band math | References |
|----|--------------------|---|------------|
| 1 | NDVI | $\frac{\text{NIR}-\text{RED}}{\text{NIR}+\text{RED}}$ | [50] |
| 2 | EVI | $G \cdot \frac{\text{NIR}-\text{RED}}{\text{NIR}+C1 \cdot \text{red}-C2 \cdot \text{Blue}+L}$ Note : C1 = 6 ; C2 = 7.5 ; L = 1 ; G = 2.5 | [49] |
| 3 | SR | $\frac{\text{NIR}}{\text{RED}}$ | [65] |
| 4 | NDI75 | $\frac{\text{RED EDGE 2}-\text{RED EDGE 1}}{\text{RED EDGE 2}+\text{RED EDGE 1}}$ | [66] |
| 5 | NDI45 | $\frac{\text{RED EDGE 1}-\text{RED}}{\text{RED EDGE 1}+\text{RED}}$ | [61] |
| 6 | IRECI | $\frac{\text{RED EDGE 3}-\text{RED}}{\text{RED EDGE 1}/\text{RED EDGE 2}}$ | [59] |

3.4.2. Pre-processing Sentinel-1 satellite image

3.4.2.1. Thermal noise removal

One of noises which appear in radar image is thermal noise. This is the addition background energy causing a noise floor. Cross-polarization (HV/VH), however, is always significantly suffered by thermal noise because their depolarized power is more weaker than their initially polarized power.

3.4.2.2. Precise orbit file

Precise orbit information is available 20 days after data acquisition. Orbit file contains the exact location of the sensor when satellite records the object. Orbit file helps to correct geolocation error of the image. Orbit file of the image is downloaded directly from SNAP 5.0 in https://qc.sentinel1.eo.esa.int/aux_poeorb/[67].

3.4.2.3. Radiometric calibration

This stage was very crucial to do as SAR data will be analyzed quantitatively. Processing terrain correction in SNAP needs beta nought (β^0) instead of sigma nought so that Digital Number (DN) was calibrated to beta nought (β^0). This process was conducted by radiometric calibration module in SNAP 5.0. Radiometric calibration in Sentinel-1 is calibrated using equation below:

$$\text{Value } (i) = \frac{|\text{DN}_i|^2}{A_i^2} \quad (6)$$

Where :

Value (i) = one of β^0 , γ^0 , σ^0 or original DN

A_i = one of beta nought (i), sigma nought(i), gamma nought (i) or DN(i)

3.4.2.4. Speckle reduction

Speckle effects or spots (looks like salt and pepper) on the SAR image are generated by the reflection of the object on the earth, interfered with the scattering of the radar signals. The speckle reduces the quality of the image so the filter speckle has to be applied. Gamma 5 x 5 filter was used for this purpose [46] [67].

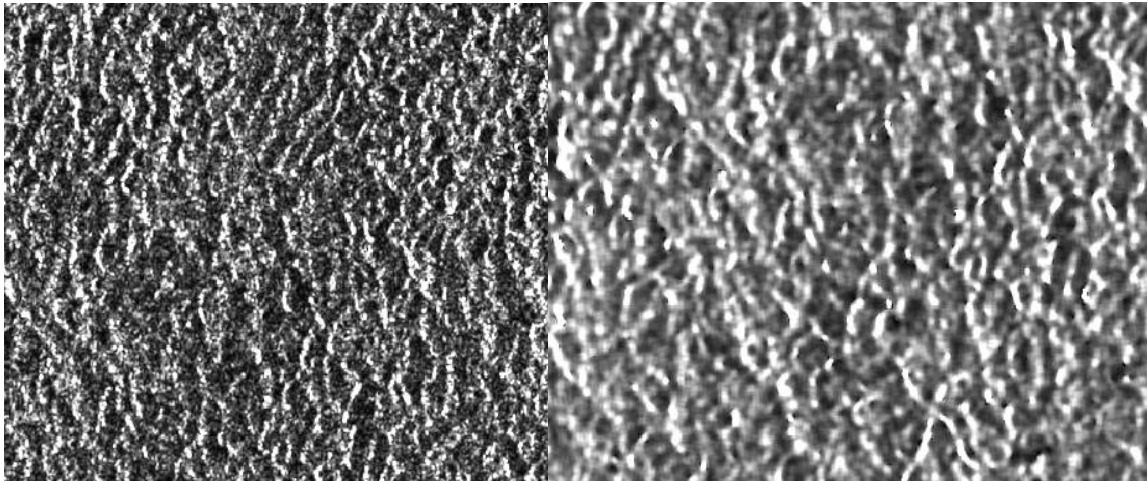


Figure 5. Speckle filtering image, Left : Sentinel-1 before speckle filtering, Right : Sentinel-1 after speckle filtering

3.4.2.5. Radiometric terrain flattening

Radiometric terrain flattening was applied because the study area has many terrain variations. Radar backscatter is strongly caused by surface roughness. If the terrain with many variations of relief (e.g. mountain and hill) face directly to the sensor, it will create small local incident angle [42]. The result of this process is brightness of the image because strong backscatter from the object to the sensor [68]. Radiometric terrain module in SNAP 5.0 converts beta nought (β°) value to gamma nought (γ°) to normalize effect of terrain on backscatter value through equation below [68].

$${}_{\gamma}T^{\circ}(r,a)=K_{\gamma} \cdot \frac{\beta^{\circ}(r,a)}{\hat{A}_{\gamma}(r,a)} \quad (7)$$

Where :

r,a = range and azimuth image coordinate

K_{γ} = scalar calibration constant

\hat{A}_{γ} = Normalization reference for gamma nought

3.4.2.6. Geometric correction

The next step of pre-processing Sentinel-1 SAR data was eliminating geometry distortion. The terrain correction processing geocoded the image by correcting geometry distortion using Digital Elevation Model (DEM) Shuttle Radar Topography Mission (SRTM) 3Sec v.4 and projected it into map coordinates. This research used the orthorectification method of Doppler Range Terrain Correction (DRTC) to eliminate geometry distortion [67]. This process produced data with pixel size of 20×20 m and projected map based on datum WGS-1984 and Universal Transverse Mercator (UTM) projection on 49 S Zone.

3.4.2.7. Converting to decibel

The value of gamma nought (γ°) was converted into decibel which is the backward scattering coefficient (backscatter). Output of this process was VV/VH backscatter values and was converted to Bean dimap in SNAP format and Geotiff format. Minchella (2015) mentioned that availability of data SAR Sentinel-1 in South

East Asia was VV/VH polarization on the Interferometric Wide Mode (IW) product [69]. IW mode captures area with 250 km swath at 5 x 20 m resolution [39].

3.5. Classification process

The private forest map of the study area was created from the Sentinel-2 image through classification process. Supervised classification was used to classify private forest and non-private forests. True colour combining red, green and blue channel was used to image enhancement. Maximum likelihood algorithm employs a bayes-family classifier to assign pixel likelihoods on the basis of mean class values as well as class covariance [70]. In order to use this algorithm, an adequate amount of pixels is needed for each sample area for the calculation of the covariance matrix. The sample areas were collected from the Sentinel-2 image via visual interpretation based on combination references between field survey result and base map from google earth.

An accuracy assessment from supervised classification of the image in each year was done. A hundred sixty Ground Control Points (GCP) were generated randomly from the field. Then, reference points were compared to the image from supervised classification results through confusion matrix to perform accuracy assessment. Overall accuracy, producer's accuracy, and user's accuracy were performed to determine accuracy of the private forest map.

3.6. Retrieval of backscatter, spectral and vegetation indices value

All of the image parameters from radar backscatter spectral value and vegetation indices was converted to geotiff format. Totally, 30 points representing coordinate of sample plots are used to retrieve the values of each image. Process to retrieve the pixel values of each image was executed in ArcGis 10.5 through extraction values to point feature. Process of retrieving pixel value of the image is illustrated by Figure 6.

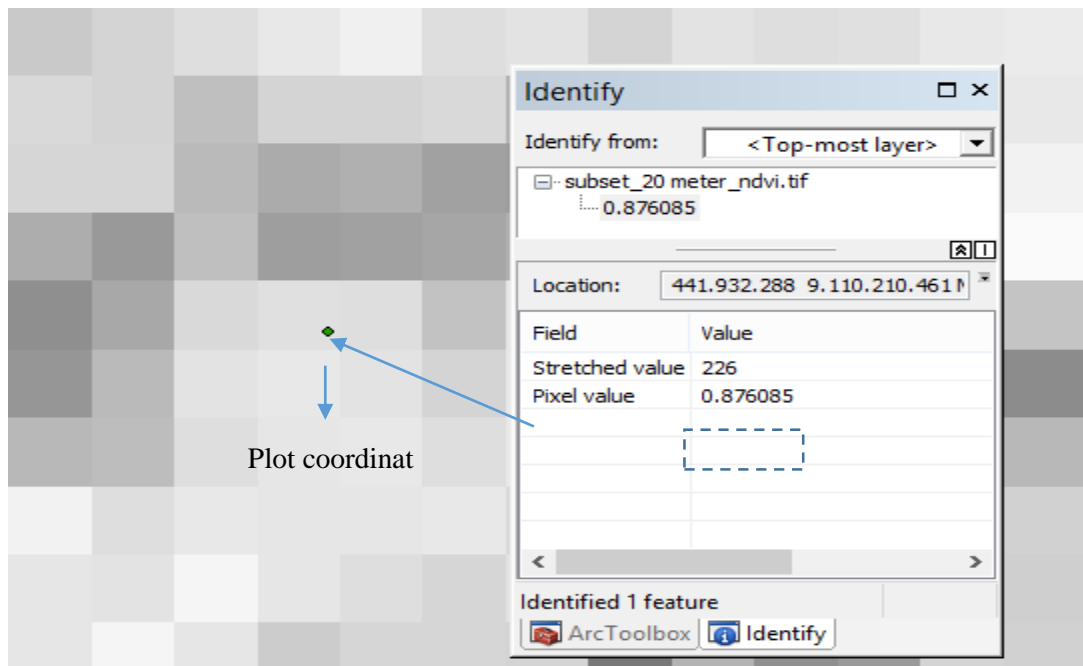


Figure 6. Retrieval pixel value from NDVI

3.7. Statistical analysis

3.7.1. Correlation analysis

Correlation analysis was the first statistical process in this research. Correlation analysis indicates the size of the correlation (relationship) or degree closeness relationship between two variables which can be between -1 and +1, where close value to -1 or +1 is strong correlation and value of 0 implies that there is no correlation between the two variables [71].

In this study, three groups of parameters were correlated. The first group was correlation between AGB of private forest and the Sentinel-1 backscatter coefficient of VV and VH image data. The second group was correlation between AGB and the Sentinel-2 spectral values which include B3, B4, B5, B6, B7 and B8 image data. The third group was correlation between AGB and vegetation indices delivered from Sentinel-2 consisting of NDI45, NDVI, SR, IRECI, NDI75 and EVI. Scatter plot between two variables were established in microsoft excel. Pearson correlation then was applied in SPSS 17 to assess correlation between AGB and parameters from Sentinel-1 and Sentinel-2.

3.7.2 Linear regression

Linear regression was used to assess the best parameters from Sentinel-1 and Sentinel-2 for estimating AGB. Similar with correlation analysis, all of the parameters was divided by three groups. AGB was considered as dependent variables and parameters from Sentinel-1 and Sentinel-2 as independent variables. Generating simple regression was using curve estimation in SPSS 17. The regression between AGB and Sentinel-1 and Sentinel-2 parameters is expressed by equation below [72] :

$$Y = a + bx \quad (8)$$

where :

Y = Dependent variable (AGB of private forest)

x = Independent variable (Sentinel-1 and Sentinel-2 parameters)

a, b = Coefficient

The best parameters was assessed through R^2 (coefficient of determination). R^2 is a measure that indicates the proportion of Y explained by X [72]. The value of R^2 is between 0 and 1 where values close to + 1 mean that parameters in X can explain almost of Y behavior. It indicates that our regression model is in fit performance [72]. Values close to 0 is the opposite in which X parameters have poor ability to explain of Y behavior.

3.7.3. Model development

AGB modelling was conducted through the stepwise linear regression model. Stepwise linear regression is combination between the forward and backward method where all output parameters in the model are tested to see their significance to the model [72]. If a non-significant parameter is detected, it will deleted from the model [72]. All of the significant parameters with AGB delivered from Sentinel-1 and Sentinel-2 was used as independent variable in this process. The equation of the multiple regression is expressed below [72]:

$$Y = a + b_1x_1 + b_2x_2 + b_3x_3 + b_nx_n \quad (9)$$

where:

Y = Dependent variable (AGB of private forest)

x = Independent variable (Sentinel-1 and Sentinel-2 parameters)

a = Intercept

b = Coefficient

The ability of the models will be assessed through R^2 (Coefficient of Determination) and Root Mean Square Error (RMSE). Equation of RMSE error is shown below:

$$\text{RMSE} = \sqrt{\frac{(Y - Y_i)^2}{n}} \quad (10)$$

where:

RMSE = Root mean square error

Y = Estimated AGB (ton/ha)

Y_i = Measured AGB (ton/ha)

n = Number of sample plots for validation

The model developed has to be free from the multicollinearity problem which can be assessed through tolerance value (>0.1) and Variance Inflation Factor (VIF) (<10) [23].

3.8. Creating AGB Map

The AGB map was created from the stepwise linear regression model. Model selected was based on high R^2 , low RMSE and fulfilling requirements of multicollinearity. The AGB map of the study area was produced through ArcGis 10.5. The process was conducted in raster calculator tools in ArcGis 10.5. Raster calculator is a tool in map algebra in spatial analysis extension. The model selected equation was entered in raster calculator. The raster calculator converted pixel value from the raster image to AGB value accordingly. Consequently, the AGB value based on the raster pixel. Negative values were masked without AGB value so that the AGB value started from 0. Then, the AGB values were classified into some groups (eg. 0-100, 100 – 150 etc.).

3.9. AGB map validation

The AGB map is very important for the user especially groups of farmers. This map can be used for replanting of private forest and helping the farmers to know the volume of their forest so they can bargain with trader. Therefore, assessing accuracy of AGB map is imperative. A fifteen sample plots as observed AGB were plotted against 15 plots as predicted AGB to validate the AGB map. R^2 and RMSE were calculated during this process.

Flow chart of the whole study is shown in Figure 7

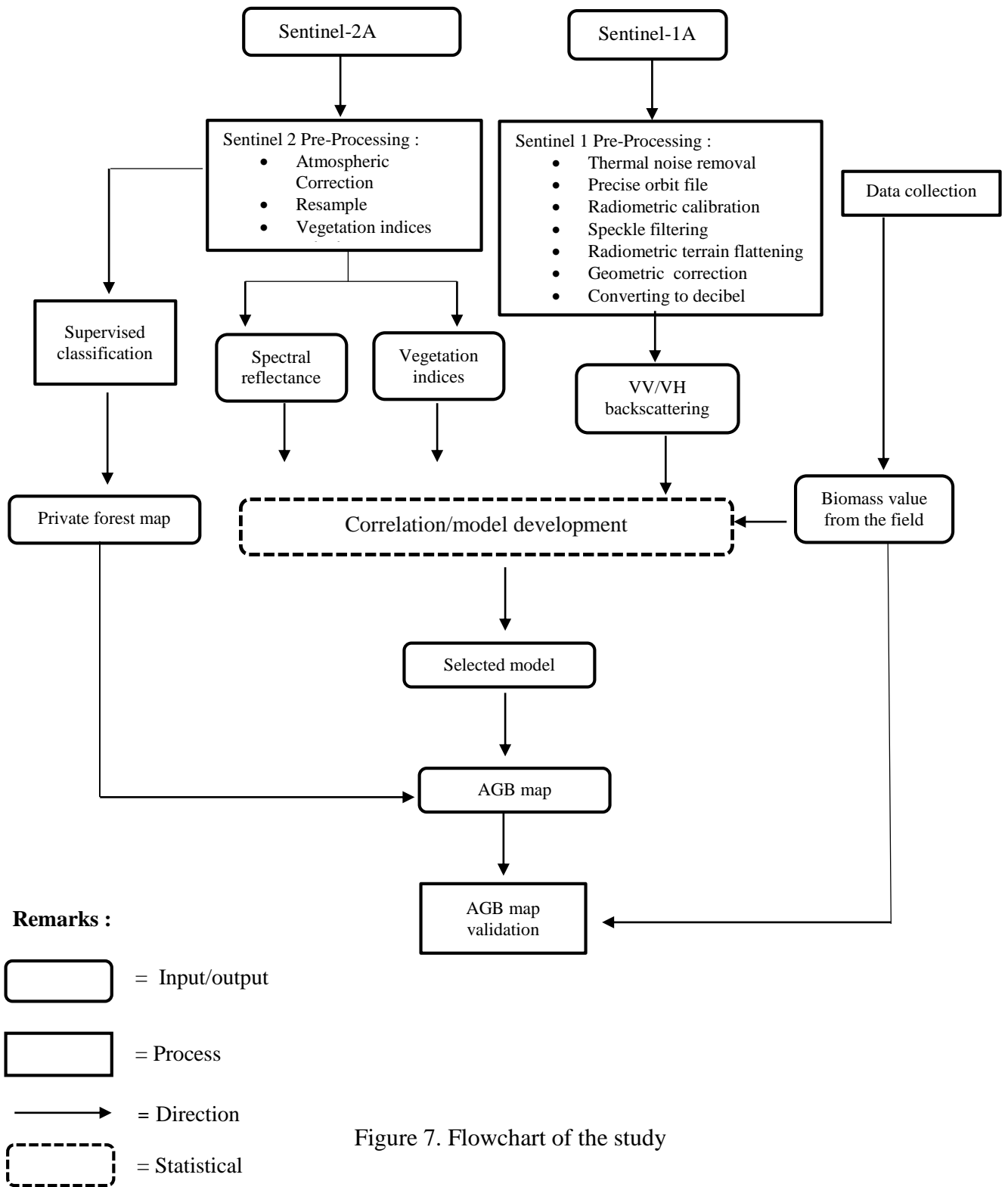


Figure 7. Flowchart of the study

CHAPTER 4

RESULT AND DISCUSSION

4.1. Descriptive analysis of field data

Forest parameters measured in the field were tree height and Diameter of Breast Height (DBH). Identification of tree species was also done in the field. A number of trees recorded in 45 (1.8 Ha) sample plots were 1,451. A total of 8 species of trees were found namely *Tectona grandis*, *Swietenia mahagony*, *Acacia auriculiformis* and other trees such as *Samanea saman*, *Gnetum gnemon*, *Alstonia scholaris*, *Parkia speciosa* and *Tamarindus indica*. The dominant species in Girisekar and Jetis forest management unit was *Tectona grandis* with a total of trees and IVI of 891 and 193.25, respectively (Table 11). The IVI for *Swietenia mahagony* and *Acacia auriculiformis*, which were being the second and third dominant species, were 54.59 and 37.22. Other tree group constituted the lowest value in term of IVI in private forest.

Table 11. Important value index for each species in this study area

| No | Species | Count | Density | RD (%) | Frequency | RF (%) | RD1(%) | IVI |
|----|------------------------------|--------------|--------------|------------|-------------|------------|------------|------------|
| 1 | <i>Tectona grandis</i> | 891 | 19.80 | 63.82 | 0.93 | 42.43 | 87.00 | 193.25 |
| 2 | <i>Swietenia mahagony</i> | 302 | 6.71 | 20.04 | 0.58 | 26.26 | 8.29 | 54.59 |
| 3 | <i>Acacia auriculiformis</i> | 232 | 5.16 | 14.45 | 0.40 | 18.18 | 4.59 | 37.22 |
| 4 | Other trees | 26 | 0.58 | 1.69 | 0.29 | 13.13 | 0.12 | 14.94 |
| | Total | 1,451 | 32.24 | 100 | 2.20 | 100 | 100 | 300 |

RD is relative density; RF is relative frequency; RD1 = relative dominance ; IVI is important value index, calculated from $RD + RF + RD1$ [73].

The field AGB of private forest was measured by plotting H and DBH allometric equations. The mean of field AGB was 80 ton/ha, with minimum and maximum values of 21 Mg/ha and 226 ton/ha, respectively. Majority of AGB plots was distributed evenly, ranging from 50 – 100 ton/ha. We found 8 sample plots with field AGB < 50 ton/ha and few sample plots with field AGB > 150 ton/ha (Figure 8). These results show that AGB value from low to medium was dominant in the study area.

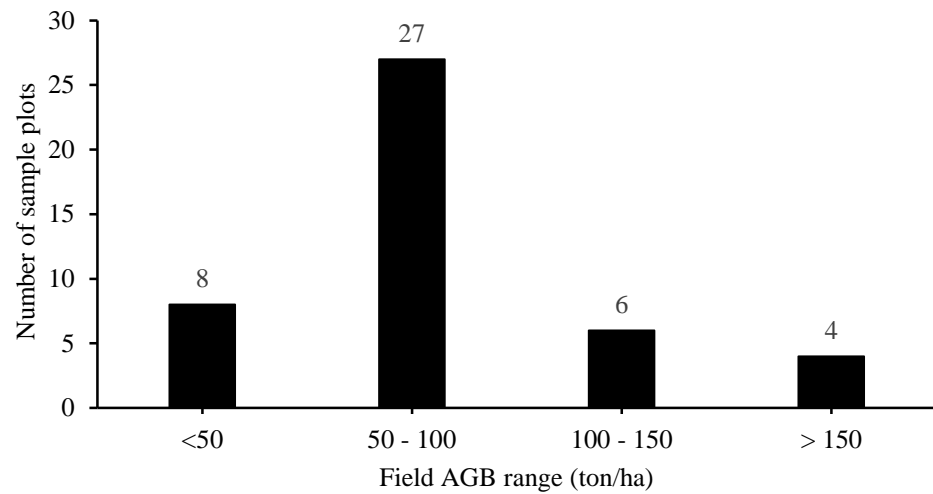


Figure 8. Distribution of field AGB within the sample plot

4.2. Private forest map

Classification was done through maximum likelihood using ENVI software. A maximum likelihood method has been widely used to classify object. In this research, two classes-forest and non-forest were set up. Non-forest included road, settlement area and water bodies. Forest area obtained by maximum likelihood classification was 1,427 Ha (Figure 9).

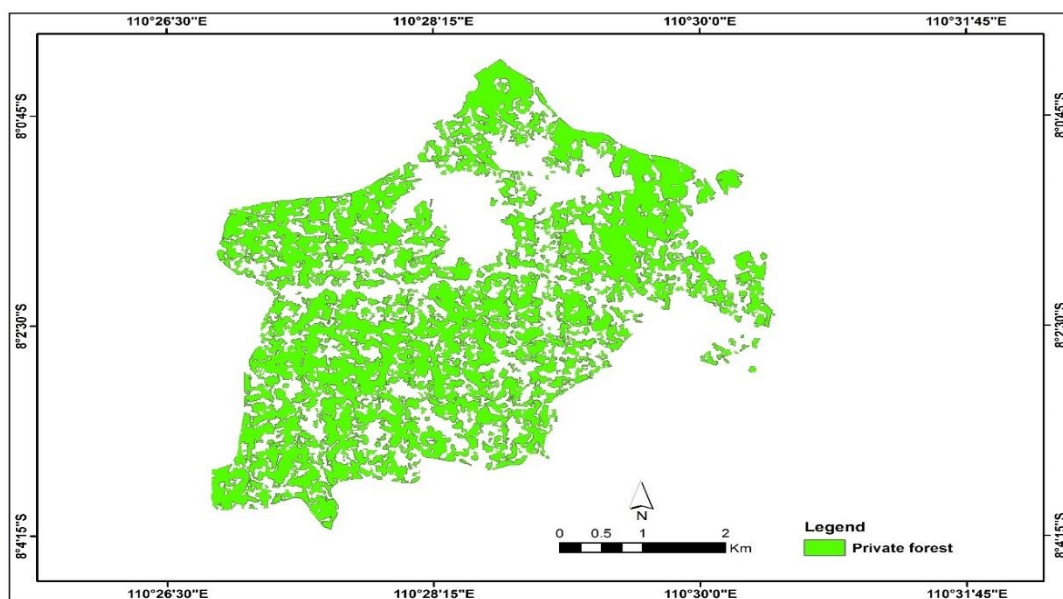


Figure 9. Private forest map unit derived from supervised classification

Post classification process was carried out to assess accuracy of private forest map. Overall accuracy, producer's accuracy and user's accuracy were set up as parameters for accuracy control that was calculated using hundred sixty ground control points. Confusion matrix was designed by comparing between ground control points and classification results. Overall accuracy, producer's accuracy, user's accuracy were calculated through confusion matrix. Finally, user's accuracy of private forest was 95 %, while producer's and overall accuracy were 95 % and 94 %, respectively.

4.3 Correlation between AGB and Sentinel-1 data

Thirty sample plots were taken from the field to establish correlation between AGB from private forest and Sentinel-1 data. Then, Pearson correlation was used to assess correlation between VV and VH Sentinel-1 polarised backscatter and AGB. VV and VH showed weak correlation to AGB where VH correlation exhibited significant relationship at 95 % confidence level, whereas VV did not correlate significantly with AGB (Table 12). The result of this study was in line with some studies who utilised C-band to assess AGB from the forest. Nizalpur et al. (2015) found that correlation between DLR-ESAR data and AGB from tropical forest in India was low ($r= 0.31$, $p\leq 0.05$) [43]. In addition, Jha et al. (2006) found similar result when they assessed correlation between AGB and Envisat-ASAR data ($r= 0.349$, $p\leq 0.05$) [21].

The weak correlation between AGB and C-band data is connected to data saturation in low AGB value. Jha et al. (2016) revealed that data saturation occurred when AGB attained 70 ton/ha [43]. A study by Imhof et al. (1995) showed that saturation level of AIRSAR data was 20 ton/ha [74]. This research showed that saturation level of Sentinel-1 SAR in VH backscatter was 50 ton/ha (Figure 10). This problem can be solved using radar data which utilise L band where it can reach saturation level up to 160 ton/ha [43]. All of the backscatter showed negative correlation with AGB which means that the AGB value increases when backscatter decreases (Figure 11). This result was confirmed by some studies which showed negative correlation between AGB and SAR data [75] [76].

Table 12. Correlation and linear regression between backscatter and AGB

| No | Paramater | <i>r</i> | <i>R</i> ² |
|----|-----------|----------|-----------------------|
| 1 | VH | -0.369* | 0.13 |
| 2 | VV | -0.238 | 0.056 |

*significant at 0.05 level

In accordance to the present results, previous studies had demonstrated that cross-polarised (HV and VH) had better correlation than co-polarised (VV and HH) [77] [78]. In addition, study from Thumaty et al. (2015) reported that HV was more stronger than HH in estimating AGB in deciduos forest in India using ALOS PALSAR [88]. Castillo et al. (2017) found that VH derived from Sentinel-1 was more robust than VV in their study for mapping AGB in mangrove forest [48].

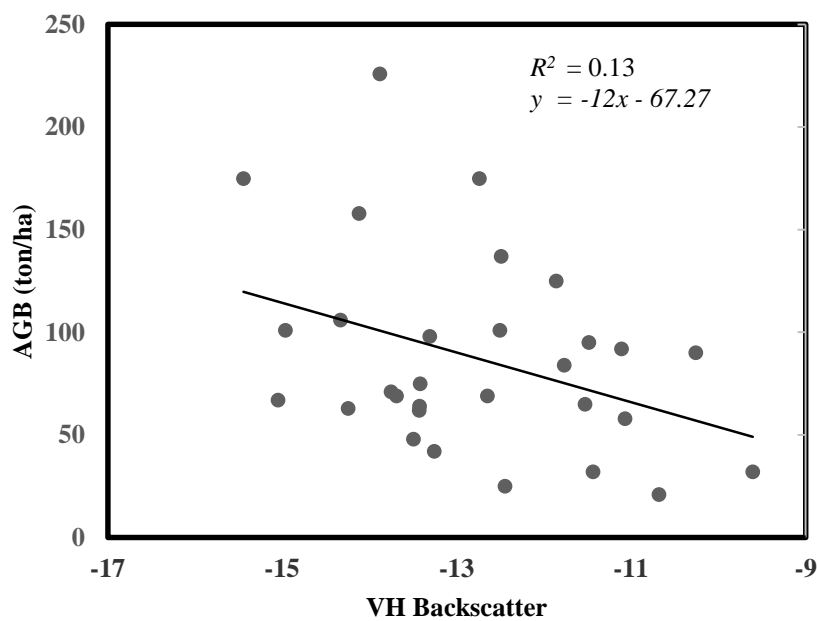


Figure 10. Scatter plot between AGB and VH backscater

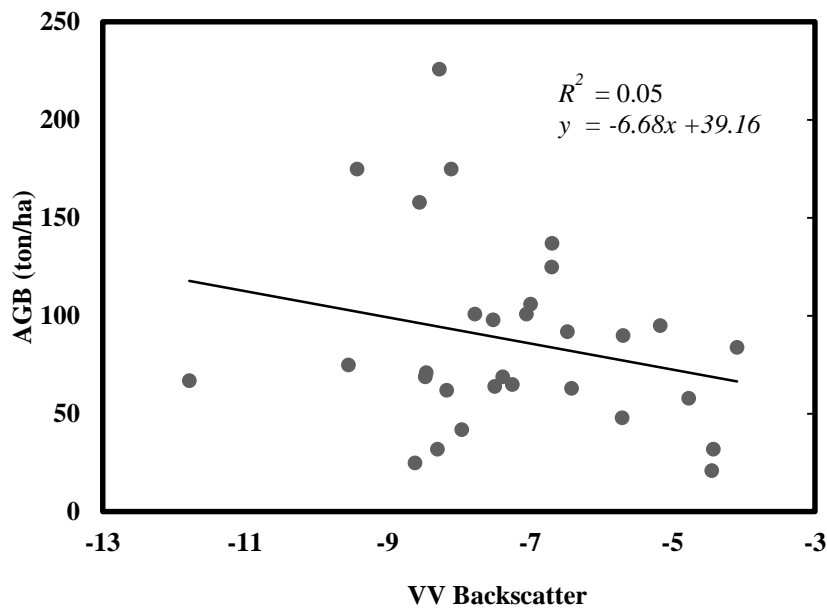


Figure 11. Scatter plot between AGB and VV backscatter

A strong correlation between VH and AGB is correlated to volume scattering. Volume scattering is the radar energy reflectance which comes from structure of canopy including small branch of trees and leaves. Tree is composed by multiple layers including leaf, brunch and trunk where reflection came from them [79]. In C-band case, cross polarisation backscatter comes from canopy leaves, secondary branch and twigs due to it has less ability to deeply penetrate through canopy [21]. On the other hand, VV backscatter only comes from surface scattering from the leaves so that returned signal to the sensor is weak. Bousbish et al. (2017) found that VH backscatter increases when the volume of the tree also increases in assesing potential of Sentinel-1 for assesing soil and cereal cover parameters [80]. This result implies that VH backscatter from the trees is volume of scattering and it will bounce back strong signal to the radar sensor.

4.4. Correlation between AGB and Sentinel-2 spectral reflectance

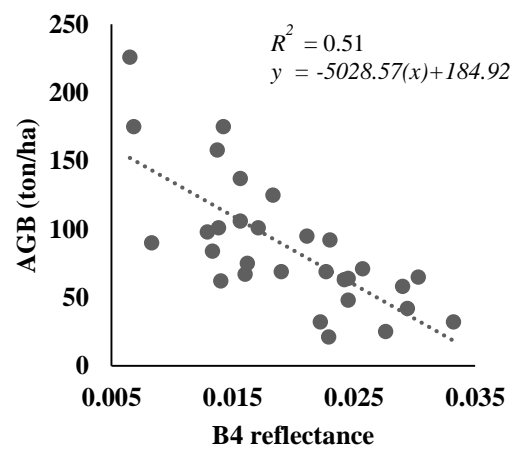
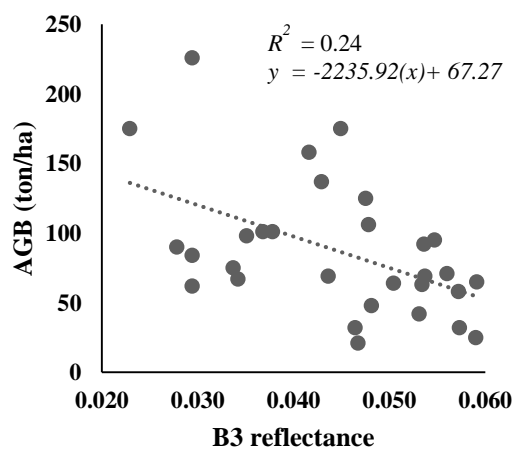
Broadband and narrow band were used to assess correlation AGB and spectral reflectance. Broadband are B3, B4 and B8, whereas narrowband are B5, B6 and B7. Table 13 presents reflectance in broadband and narrowband in relation to AGB in private forest. B4 appeared as stronger and better parameter than others Sentinel-2 bands. In contrary, there was a non significant correlation between AGB and B5-B8. On the other hand, B3 showed moderate correlation to AGB.

The spectral reflectance showed both positive and negative correlation to AGB. B3, B4 and B5 exhibited negative correlation to AGB which means that the value of AGB increases when the value of spectral reflectance decreases (Figure 12). Positive correlation to AGB was showed by B6, B7 and B8 and it concluded that AGB value will increase when the value of spectral reflectance increases.

Table 13. Correlation and linear regression between spectral reflectance and AGB

| No | Parameters | <i>r</i> | <i>R</i> ² |
|----|------------|----------|-----------------------|
| 1 | B3 | -0.50* | 0.24 |
| 2 | B4 | -0.73* | 0.51 |
| 3 | B5 | -0.33 | 0.11 |
| 4 | B6 | 0.20 | 0.04 |
| 5 | B7 | 0.30 | 0.09 |
| 6 | B8 | 0.24 | 0.06 |

*significant at 0.05 level



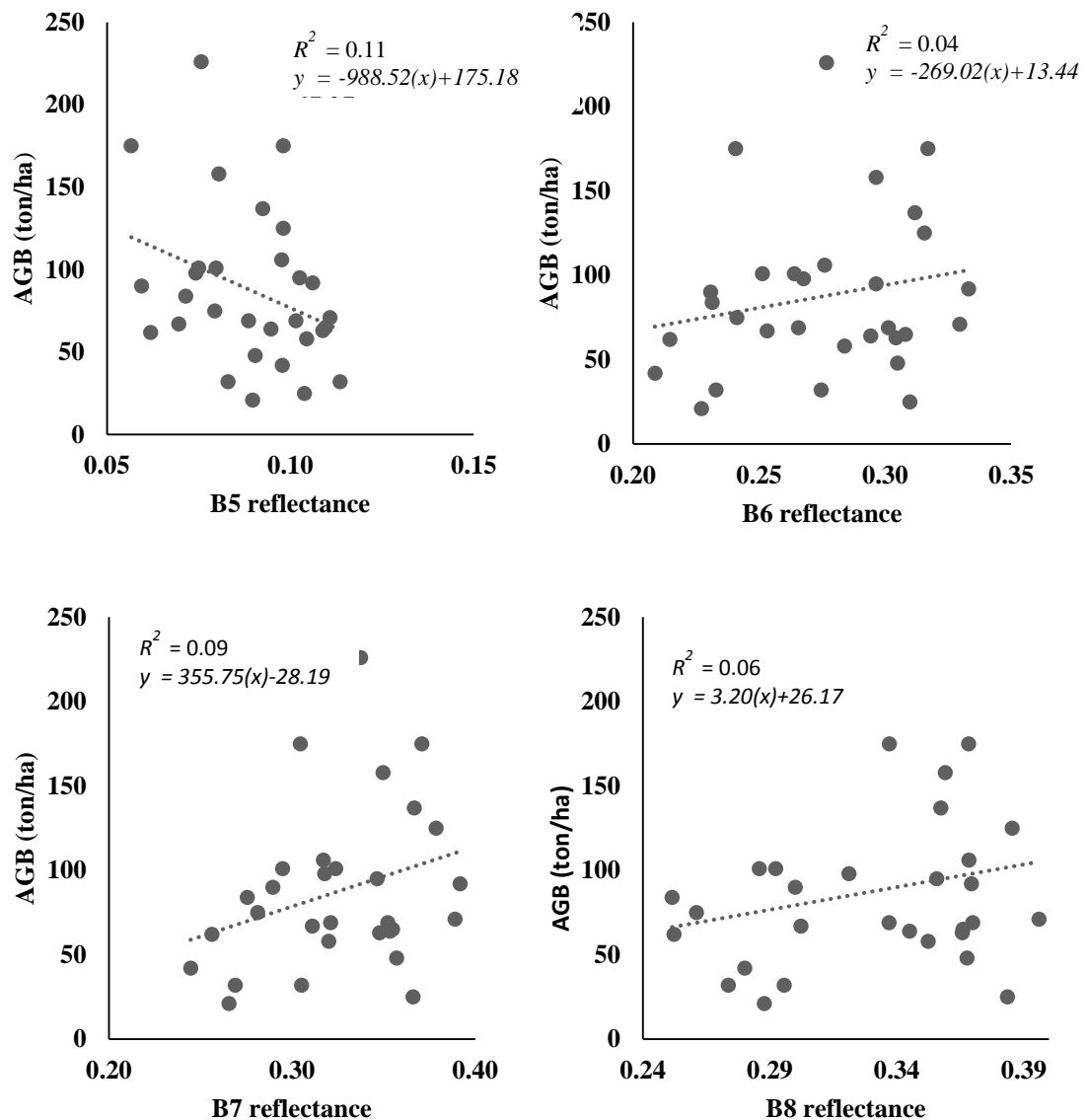


Figure 12. Scatter plot between AGB and spectral reflectance

Several studies have shown that NIR is band known to have good correlation with biomass [81] [48]. It is reasonable since it can be correlated to high reflectance of NIR region from healthy vegetation. However, the finding of the current study does not support the previous research. From the Table 13, it can be seen that red is better than other bands in estimating AGB on private forest. This result agreed with the findings of other studies, in which red is more robust than NIR to assess biophysics parameters of the vegetation [82] [83]. For example, Pu et al. (2015) found that correlation between red and LAI was stronger than NIR in mapping LAI forest area in USA [82]. Gomez et

al. (2012) utilised spectral values derived from QuickBird-2 image to predict forest structural properties and they revealed that the red reflectance was more robust than NIR [83].

Another finding in this research was red edge bands did not have good correlation to AGB in private forest. This finding corroborates the result from Pu et al. (2015), who found that visible bands was stronger than red edge bands [82]. Furthermore, they added that small variation of red edge reflectance because of narrow range did not match with large variation in LAI in mixed forest [82]. This explanation supports the result of this study where our study site was composed by mixed plantation (Table 11) so that it produced many variations of LAI value. Dussuex et al. (2015) found that LAI is more correlated to AGB than other biophysical parameters of the vegetation [84].

4.5. Correlation between AGB and vegetation indices

Result of linear regression analysis between AGB and vegetation indices derived from Sentinel-2 are shown in Table 14. The r value of vegetation indices was ranging from 0.49 to 0.89 and R^2 varied between 0.23 and 0.79. All of vegetation indices showed significant and positive correlation with AGB. NDI45 was the best vegetation indices corresponded to AGB ($r = 0.89$ and $R^2 = 0.79$) followed by SR, NDVI, IRECI, NDI75 and EVI

Table 14. Correlation and linear regression between vegetation indices and AGB

| No | Parameters | r | R^2 |
|----|------------|--------|-------|
| 1 | NDI45 | 0.89** | 0.79 |
| 2 | NDVI | 0.81** | 0.65 |
| 3 | IRECI | 0.7** | 0.49 |
| 4 | SR | 0.86** | 0.73 |
| 5 | EVI | 0.49** | 0.23 |
| 6 | NDI75 | 0.62** | 0.38 |

*significant at 0.05 level

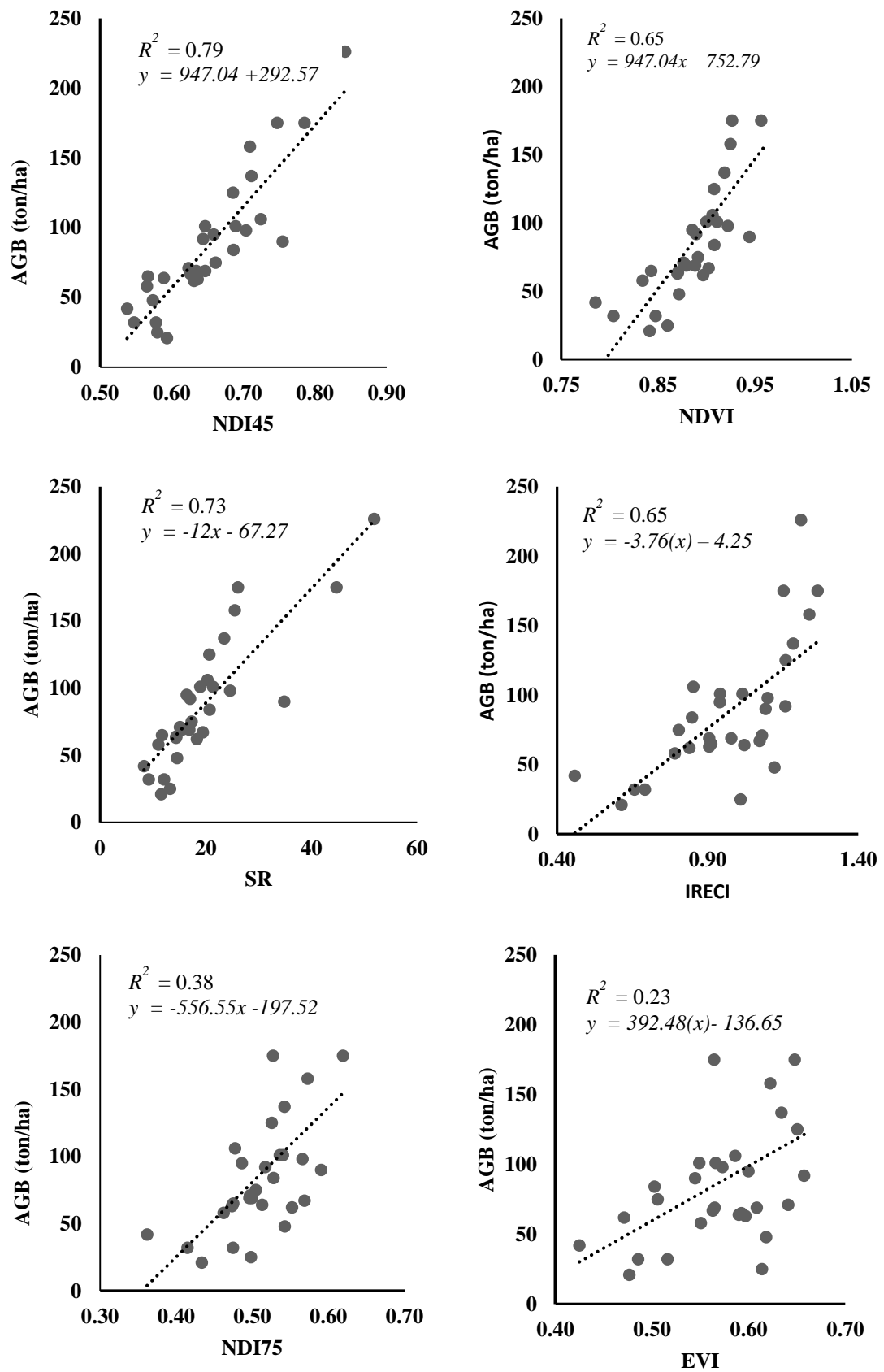


Figure 13. Scatter plot between AGB and vegetation indices

Pearson correlation was employed for assessing the relationship between AGB and vegetation indices derived from Sentinel-2 image. NDI45, SR and NDVI had strong correlation with AGB. NDVI is most widely used to measure biophysics properties of vegetation. So, we compared it with other indices on this research. Once NDI45 and NDVI was compared, NDI45 was more powerful than NDVI since NDVI had a saturation problem at a higher value of biomass (Figure 13). A possible explanation for this result may be linked to the lower saturation of high AGB level of red edge 1 compared to the NIR band (Table 13).

A substitute of NIR to the red edge 1 on NDI45 at Sentinel-2 image is able to improve relationship between satellite data and biophysics properties of the vegetation. This is consistent with the result of Frampton et al. (2013) where correlation between NDI45 was higher than NDVI in measuring Canopy Chlorophyll Content (CCC) [59]. NDI45 created from Sentinel-2 B4 (665 nm) and red edge 1 B5 (705 nm) is more robust to measure biophysics parameters of vegetation than other bands combination in Sentinel-2 [61].

SR outperformed NDVI in this study. It might be because the relationship of MSR and SR with biophysical properties of the vegetation was more linear than NDVI [59] [65]. NDVI is more affected by leaf optical and geometry effect from sun view angle hence linearity to parameters of vegetation is lower than SR [65]. EVI is more reliable than NDVI to measure AGB on dense vegetation because its ability to reduce effect of atmosphere and canopy background. However, EVI showed poor correlation to AGB in this research. A possible explanation is that the slope of the plots in the study area varies from flat to slightly inclined (slopes range of the sample plots between 0° to 19°). EVI is highly influenced by various terrain condition [84] [85]. Soil adjustment factor (L) becomes limitation of EVI because it is very sensitive to topography than indices which are based on simple ratio algorithm like SR and NDVI [85].

4.6. Modelling AGB in private forest

Having reliable AGB values are important to effectively produce an AGB map. The AGB map can be derived from modelling between satellite data and AGB from field measurement. Regression model has been widely used to modelling AGB and

satellite image data [14], [16], [54]. Regression model is used to model relationship between independent variables (x) and dependent variable (y).

Stepwise multilinear linear regression was used to estimate AGB in private forest. This model uses more than one independent variables. In this case, all of the significant variables from Sentinel-1 and Sentinel-2 was plotted as independent variables and AGB as a dependent variable. The summary output of the model is presented in Table 15.

Table 15. Summary of paramaters for AGB model development

| Sensor | Parameters |
|------------|--------------------------------------|
| Sentinel-1 | Gamma VH |
| Sentinel-2 | B3,B4, NDI45,SR,NDVI,IRECI,NDI75,EVI |

Based on stepwise linear regression, combination between NDI45 and EVI appeared as better parameters combination to establish AGB model in private forest. A developed model from NDI45 and EVI fitted for estimating AGB (adjusted $R^2 = 0.81$, $p < 0.05$). R^2 81 % means that as much as 81 % of AGB variability could be explained. AGB model for private forest is expressed by formula below :

$$AGB = (537 * NDI45) + (158.42 * EVI) - 353.66 \quad (11)$$

VIF and Tolerance value for model was 0.87 and 1.14, respectively. It suggested that there was no multicollinearity problem because tolerance value was more than 0.1 and VIF value was less than 10 [23]. RMSE of the model was 19.4 ton/ha. Thus, this model was accepted for estimating AGB private forest.

4.7. AGB Map validation

Model validation was employed to assess performance of the model. Lu et al. (2016) stated that RMSE and R^2 commonly are used to validate AGB. Two groups of data were choosen, namely observed and predicted AGB. Observed AGB was derived from field AGB and predicted AGB was obtained from the AGB map using fiveteen sample plots from the field. Finally, simple linear regression has been developed from the data to validate the model. Realibility of the model is determined by low RMSE and high R^2 [15].

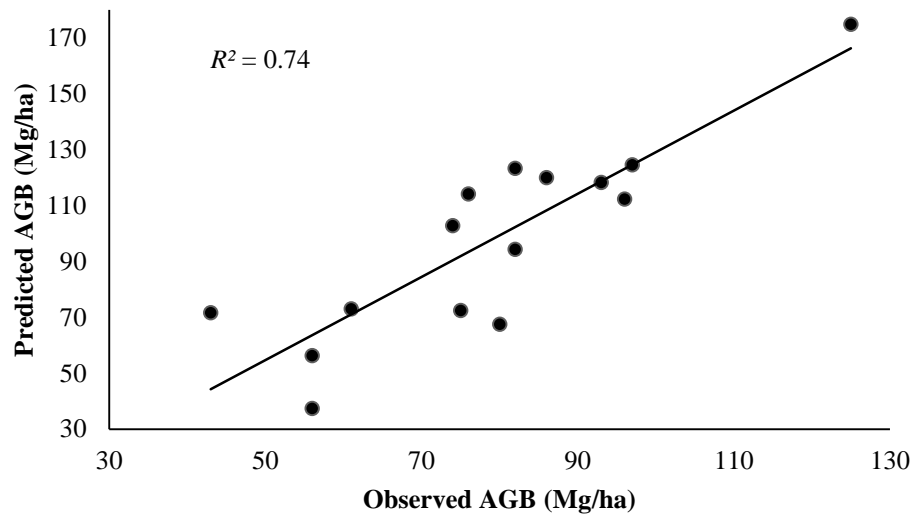


Figure 14. Scatter plot of observed and predicted AGB

Correlation between observed and predicted AGB gave a robust R^2 , 0.74. It means that 74 % of observed AGB could be explained by predicted AGB. The regression analysis results of the the model validation are highlighted in equation 12. The scatter plot of the validation model is presented in Figure 14.

$$Y = -29.85 + 0.50x \quad (12)$$

Where :

Y = observed AGB (ton/ha)

X = predicted AGB (ton/ha)

RMSE obtained from predicted and observed AGB was 27 ton/ha. In accordance to this result, some previous studies resulted RMSE lower than 27 ton/ha [23] [14] [87]. For example, Hamdan et al. (2014) estimated AGB in Malaysia where they obtained RMSE of 32.57 ton/ha [14]. Futhermore, Jackowsky et al. (2013) predicted AGB in mangrove forest in Southern Thailand using WorldView-2 and found that RMSE error of AGB model was 53.4 ton/ha [87]. However, this result different from some published studies who found that RMSE more than 27 ton/ha [88] [89]. Thumaty et al. (2016) reported RMSE in estimating AGB in deciduos forest in India using ALOS PALSAR was 19.31 ton/ha [88]. It indicated that RMSE result of this study was moderate and reasonable to predict AGB in private forest.

4.8. Mapping AGB in private forest

Estimating AGB in the study area was conducted using equation 11. The process was done in ArcGIS 10.5 using map algebra. The equation which was obtained from stepwise linear regression was typed in raster calculator to extrapolate AGB map. Due to NDI45 and EVI are the x variable in the equation, the software calculates AGB directly based on the pixel value. Output in this process is raster AGB map where each raster pixel contains AGB values. This method also was used by Castillo et al. (2016) who estimated AGB in their study area using raster calculator in ArcGIS [48]. The AGB map of the study area is illustrated in Figure 15.

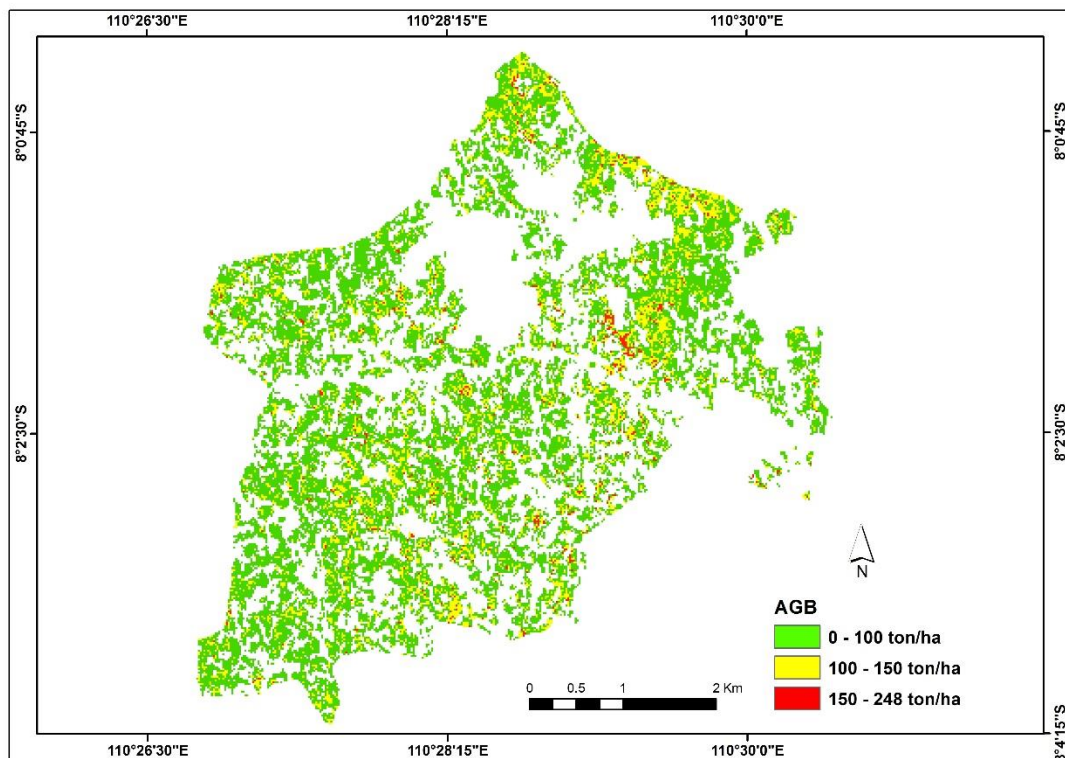


Figure 15. AGB map of the study area

Figure 15 illustrates AGB map prediction resulted from the stepwise linear regression model between AGB field and vegetation indices (NDI 45 and EVI). The number of AGB predicted for Girisekar and Jetis private forest management unit from spatial analysis was 72.54 ton/ha. The AGB values varied from 0 – 248 ton/ha. Using

0.5 conversion factor from biomass to carbon, above ground carbon biomass estimated from the study area was 36.27 ton/ha.

Table 16. Summary of AGB estimating in private forest

| No | Methodology | Location | Mean AGB (ton/ha) | References |
|----|----------------------|------------------------|-------------------|------------|
| 1 | Forest Inventory | Ngaleran, Yogyakarta | 38.1 | [90] |
| 2 | Destructive sampling | Dengok, Yogyakarta | 49 | [91] |
| 3 | Remote sensing | Girisekar, Yogyakarta | 72.54 | This study |
| 4 | Forest Inventory | Terong, Yogyakarta | 64.42 | [92] |
| 5 | Forest Inventory | Rejomakmur, Yogyakarta | 75.31 | [64] |

This research found that AGB derived from remote sensing method was moderate. To ensure that our result is validated, comparing with another research in estimating AGB in private forest is imperative. Because the number of literature for estimating AGB in private forest using remote sensing method was limited, so we utilised others research using different methods as comparison (Table 16). The AGB value of this research is almost similar to AGB value (75.31 ton/ha) reported by Arupa in Rejomakmur but higher than the AGB value who found by Aminuddin (49 ton/ha) in Dengok and Arupa (64 ton/ha) in Terong. The AGB value of this study almost double than AGB value (38.1 ton/ha) from Ngaleran who was estimated by Purwanto et al. (2015) [90].

AGB value in private forest can be categorised as moderate AGB. The number of AGB in private forest is lower than AGB from some forest types like natural forest [81] and mangrove [87]. For instance, Wijaya et al. (2009) conducted research in Borneo and found that AGB value in secondary primary forest was 167 ton/ha [81]. However, AGB in private forest is higher than those from deciduous forest in India which was estimated by Thumaty (58 ton/ha) [88]. The lower of AGB can be linked to traditional philosophy that considers private forest as a long-term investment. It means that private forest can be used intentionally (*tebang butuh* on local language). Farmers usually will harvest timber of private forest in particular time such as the start of school

year and wedding event. Therefore, the average of field AGB was 80 ton/ha where only one sample plot had field AGB more than 200 ton/ha and the others below 200 ton/ha. It is too difficult to find areas with high AGB value on private forest because the farmers harvest mature trees. So, it is plausible if majority of the sample plots would be only in low to medium AGB areas.

CHAPTER 5

CONCLUSION

This study explored the potential of Sentinel-1 and Sentinel-2 satellite data to quantify above ground biomass in Girisekar and Jetis forest management unit, Yogyakarta, Indonesia. Pearson correlation and single linear regression were used to assess correlation between AGB and satellite data. AGB modelling from private forest then was derived using stepwise linear regression. The conclusion of this study is as follows :

1. Sentinel-1 backscatter (VV and VH) showed low correlation with AGB because of data saturation of C-band. The accuracy of VH for capturing AGB was significantly better than VV.
2. Broad band from Sentinel-2 which consists of B3 and B4 was better than NIR red edge band in retrieving AGB in private forest.
3. Vegetation indices from Sentinel-2 appeared as strong parameters than reflectance from Sentinel-2 band and Sentinel-1 band backscatter. All of the vegetation indices which were used in this research showed significant correlation to AGB where NDI45 was much better than other indices.
4. Model of Girisekar and Jetis private forest derived from stepwise linear regression found that combination between NDI45 and EVI was more robust ($R^2 = 0.81$). The model can be written as follow:

$$AGB = (537 * NDI45) + (158.42 * EVI) - 353.66$$
5. The mean of AGB in study area was 72.54 ton/ha. Model validation result showed that it can perform well in the study area (RMSE = 27 ton/ha). Based on the literature review comparison, the mean of AGB was relatively close to AGB value in other research areas which have same characteristics to our study area.
6. This research focused on private forest cultivated by the farmers in their own land. In the future, the methodology in this research can be tested in the other types of forest or agricultural plantations like rubber tree. Moreover, this research utilised free and low cost satellite like Sentinel-1 and Sentinel -2 and their own software,

SNAP. This is important to developing countries or researchers which have limitation for satellite purchasing.

7. The limitations of this research was few sample plots in high AGB area with the mean of AGB field of 80 ton/Ha. It implicated satisfying statistic result because the model was less affected by data saturation especially in Sentinel-2 image. There is available room in the future to test ability of Sentinel-2 in the area which has high AGB value such as natural forest so that the potential of Sentinel-2 can be explored deeply.

REFERENCES

- [1] FAO (Food and Agriculture Organization), “Forests and Climate Change Working Paper 5: Definitional issues related to reducing emissions from deforestation in developing countries.” FAO, 2007.
- [2] B. A. Margono, P. V. Potapov, S. Turubanova, F. Stolle, and M. C. Hansen, “Primary forest cover loss in indonesia over 2000-2012,” *Nat. Clim. Change*, vol. 4, no. 8, pp. 730–735, 2014.
- [3] M. C. Hansen, S. V. Stehman, P. V. Potapov, B. Arunarwati, F. Stolle, and K. Pittman, “Quantifying changes in the rates of forest clearing in Indonesia from 1990 to 2005 using remotely sensed data sets,” *Environ. Res. Lett.*, vol. 4, no. 3, p. 034001, 2009.
- [4] Forest Watch Indonesia and Global Forest Watch, *The state of the Forest: Indonesia*. Bogor, Indonesia: Forest Watch Indonesia, 2002.
- [5] World Bank, *Indonesia and Climate Change: Current Status and Policies*. Indonesia: World Bank, 2007.
- [6] Kementerian Lingkungan Hidup dan Kehutanan Indonesia, *Statistik Kementerian Lingkungan Hidup dan Kehutanan Indonesia 2015*. Jakarta, 2016.
- [7] Republik of Indonesia, “Intended Nationally Contribution Republik of Indonesia.” Jakarta, 2015.
- [8] MFP (Multistakeholder Forestry Programme, “strategi percepatan perluasan akses kelola Masyarakat atas kawasan hutan negara,” Jakarta, 2015.
- [9] Direktorat Penyiapan Kawasan dan Usaha Perhutanan Sosial, *Rencana Strategis Direktorat Penyiapan Kawasan Perhutanan Sosial Tahun 2015 - 2019*. Jakarta: Kementerian Lingkungan Hidup dan Kehutanan Republik Indonesia, 2015.
- [10] Forestry Department of FAO, “Global forest resources assesment 2010 : term and definition.” FAO, 2010.
- [11] Center For International Forestry Research, “Info Brief: Mendorong usaha tanaman kayu sebagai bisnis yang menarik bagi petani.” Cifor, 2015.
- [12] L. Goers, J. Lawson, and E. Garen, “Economic Drivers of Tropical Deforestation for Agriculture,” in *Managing Forest Carbon in a Changing Climate*, M. S. Ashton, M. L. Tyrrell, D. Spalding, and B. Gentry, Eds. Springer Netherlands, 2012, pp. 305–320.
- [13] T. Tokola, ‘Remote Sensing Concepts and Their Applicability in REDD+ Monitoring’, *Curr. For. Rep.*, vol. 1, no. 4, pp. 252–260, 2015.
- [14] O. Hamdan, I. M. Hasmadi, and H. K. Aziz, “Combination of SPOT-5 and ALOS PALSAR images in estimating aboveground biomass of lowland Dipterocarp forest,” *IOP Conf. Ser. Earth Environ. Sci.*, vol. 18, no. 1, p. 012016, 2014.
- [15] Dengsheng lu, “The potensil and challenge of remote sensing - based biomas estimation,” *Int. J. Remote Sens.*, pp. 1297–1328, 2016.
- [16] A. A. Wani, P. K. Joshi, and O. Singh, “Estimating biomass and carbon mitigation of temperate coniferous forests using spectral modeling and field inventory data,” *Ecol. Inform.*, vol. 25, pp. 63–70, 2015.

- [17] C. Huang, X. Ye, C. Deng, Z. Zhang, and Z. Wan, "Mapping Above-Ground Biomass by Integrating Optical and SAR Imagery: A Case Study of Xixi National Wetland Park, China," *Remote Sens.*, vol. 8, no. 8, p. 647, 2016.
- [18] M. F. C. Pedro W.M.Souza-Filho, A. q silva Marcus E.B. Fernandes, J. R. D. S. Maria R.S Abreu, and W. R. N. Marc Simard, "Radarsat-2 Backscattering for the Modelling if Biophysical Parameters og Regenerating Mangrove Forest," *MDPI*, pp. 17098–17112, 2015.
- [19] N. G. Mahmud Reza Sahebi and Ali Mohammadzadeh, "A review on biomass estimation methods using synthetic aperture radar data," *Int. J. Geomat. Geosci.*, vol. 1 No. 4, pp. 776–778, 2011.
- [20] H. Omar, M. H. Ismail, K. A. Hamzah, N. Kamarudin, and H. Z. Mohd Shafri, "Factors affecting L-band Alos Palsar backscatter on tropical forest biomass," *Glob. J. Sci. Front. Res. Agric. Vet.*, vol. 14, no. 3, pp. 51–64, 2014.
- [21] C. S. Jha, M. Rangaswamy, N. Vyjayanthi, and M. S. R. Murthy, "Estimation of forest biomass using Envisat-ASAR data," vol. 6410, pp. 641002–641002–8, 2006.
- [22] M. N. Kilaparti Kumar, K. K. Apichon Witayangkurn, and Shinichi Nakamura, "Above Ground Biomass assesment from Combined Optical and SAR Remote Sensing Data in Shurat Tahni Province, Thailand," *Journal Geogr. Inf. Syst.*, pp. 506–516, 2016.
- [23] S. Eckert, "Improved Forest Biomass and Carbon Estimations Using Texture Measures from WorldView-2 Satellite Data," *Remote Sens.*, vol. 4, no. 4, pp. 810–829, 2012.
- [24] G. M. Foody, D. S. Boyd, and M. E. J. Cutler, "Predictive relations of tropical forest biomass from Landsat TM data and their transferability between regions," *Remote Sens. Environ.*, vol. 85, no. 4, pp. 463–474, 2003.
- [25] P. Vicharnakorn, R. P. Shrestha, M. Nagai, A. P. Salam, and S. Kiratiprayoon, "Carbon Stock Assessment Using Remote Sensing and Forest Inventory Data in Savannakhet, Lao PDR," *Remote Sens.*, vol. 6, no. 6, pp. 5452–5479, 2014.
- [26] Indonesian Government, "Undang - undang Republik Indonesia Nomor 41 tahun 1999 tentang kehutanan." 1999.
- [27] "Tinjauan tentang pola tanam hutan rakyat," Online [Available] : <http://dishut.jabarprov.go.id/images/.../TINJAUAN%20TENTANG%20POLA%20OTANAM>. [Accessed: 25-Apr-2017]
- [28] T. Puspitojati, M. Y. Mile, F. Eva, and D. Darusman, *Hutan rakyat : Sumbangsih Masyarakat Pedesaan Untuk Hutan tanaman*. Bogor: Pusat Penelitian dan Pengembangan Perubahan Iklim dan Kebijakan, Kementerian Kehutanan, 2014.
- [29] Sandra Brown, *Estimating Biomass and Biomass Change of Tropical Forest. a Primer* (FAO Forestry Paper), 1997.
- [30] Tim perubahan iklim, badan litbang kehutanan, *Carbon stock on various type of forest and vegetation in Indonesia*. Pusat penelitian dan pengembangan perubahan iklim dan kebijakan, Kementerian Kehutanan, 2010.
- [31] X. Zhang, Y. Zhao, M. S. Ashton, and X. Lee, "Measuring Carbon in Forests," in *Managing Forest Carbon in a Changing Climate*, M. S. Ashton, M. L. Tyrrell, D. Spalding, and B. Gentry, Eds. Springer Netherlands, 2012, pp. 139–164.
- [32] K. Meister, M. S. Ashton, D. Craven, and H. Griscom, "Carbon Dynamics of Tropical Forests," in *Managing Forest Carbon in a Changing Climate*, M. S.

- Ashton, M. L. Tyrrell, D. Spalding, and B. Gentry, Eds. Springer Netherlands, 2012, pp. 51–75.
- [33] Irvin K. Samalca, *Estimation of Forest Biomass and its Error*. International Institute for Geo-Information and Earth observation, 2007.
- [34] H. K. Gibbs, S. Brown, J. O. Nilsson, and J. A. Foley, “Monitoring and estimating tropical forest carbon stocks: making REDD a reality,” *Environ. Res. Lett.*, vol. 2, no. 4, p. 045023, 2007.
- [35] “Academic paper (PDF): Review of the use of remote sensing for biomass estimation to support renewable energy generation,” *ResearchGate*. [Online]. Available: https://www.researchgate.net/publication/281426044_Review_of_the_use_of_remote_sensing_for_biomass_estimation_to_support_renewable_energy_generation. [Accessed: 06-Apr-2017].
- [36] S. Brown, “Measuring carbon in forests: current status and future challenges,” *Environ. Pollut.*, vol. 116, no. 3, pp. 363–372, 2002.
- [37] Xin Zhang, Yong Zhao, Mark S. Ashton, and Xuhui Lee, “Measuring carbon in forest,” in *Managing Forest Carbon in a Changing Climate*, USA: Springer, 2012, p. 357.
- [38] T. M. Basuki, P. E. van Laake, A. K. Skidmore, and Y. A. Hussin, “Allometric equations for estimating the above-ground biomass in tropical lowland Dipterocarp forests,” *For. Ecol. Manag.*, vol. 257, no. 8, pp. 1684–1694, 2009.
- [39] J. Návar, “Allometric equations for tree species and carbon stocks for forests of northwestern Mexico,” *For. Ecol. Manag.*, vol. 257, no. 2, pp. 427–434, 2009.
- [40] B. W. Nelson, R. Mesquita, J. L. G. Pereira, S. Garcia Aquino de Souza, G. Teixeira Batista, and L. Bovino Couto, “Allometric regressions for improved estimate of secondary forest biomass in the central Amazon,” *For. Ecol. Manag.*, vol. 117, no. 1, pp. 149–167, 1999.
- [41] T. Lillesand, Ralph Kiefer, and Jonathan Chipman, *Remote sensing and image interpretation*, Sixth. United States Of America: John Wiley & Sons, 2008.
- [42] A Canada Centre for Remote Sensing Tutorial, *Fundamentals of remote sensing*. Canada: A Canada Centre for Remote Sensing Tutorial, 2012.
- [43] V. N. Chandra Sekhar Jha and Rangaswamy Magudu, “Estimation of above ground biomass in Indian tropical forested area using multifrequency DLR-ESAR data,” *Int. J. Geomat. Geosci.*, vol. 1 No. 2, pp. 167–178, 2010.
- [44] *Sentinel 1 Hand book*, vol. 01. ESA (European space agency), 2013.
- [45] N. Torbick, D. Chowdhury, W. Salas, and J. Qi, “Monitoring rice agriculture across Myanmar using time series Sentinel-1 assisted by Landsat-8 and PALSAR-2,” *Remote Sens.*, vol. 9, no. 2, 2017.
- [46] S. Abdikan, F. B. Sanli, M. Ustuner, and F. Calò, “Land cover mapping using Sentinel-1 SAR data,” *Int. Arch. Photogramm. Remote Sens. Spat. Inf. Sci.*, vol. XLI-B7, 2016, no. 2016, pp. 757–761, 2016.
- [47] A. A. Bayayuddin, “Pendugaan Cadangan Karbon di Atas Permukaan Pada Hutan Rakyat Dengan Memanfaatkan Data Synthetic Aperture Radar Sentinel-1 (studi kasus di kabupaten Sukoharjo),” *Muhammadiyah University Surak.*, 2016.
- [48] J. Alan Castillo, A. Apan, M. Tek, and S. Salmo III, “Using Sentinel Imagery in Modelling the Aboveground Biomass of Mangrove Forest and their Competing Land Uses.” 2016.

- [49] A. Huete, K. Didan, T. Miura, E. P. Rodriguez, X. Gao, and L. G. Ferreira, "Overview of the radiometric and biophysical performance of the MODIS vegetation indices," *Remote Sens. Environ.*, vol. 83, no. 1–2, pp. 195–213, 2002.
- [50] C. J. Tucker, "Red and photographic infrared linear combinations for monitoring vegetation," *Remote Sens. Environ.*, pp. 127–150, 1979.
- [51] J. Qu, A. R. Huete, Y. . Kerr, and S. Sorooshian, "A modified soil adjust vegetation index," *Remote Sens Env.*, pp. 119–126, 1994.
- [52] B. Pinty and M. M. Verstraete, "GEMI: A Non-Linear Index to Monitor Global Vegetation from Satellites," *Vegetatio*, vol. 101, no. 1, pp. 15–20, 1992.
- [53] G. M. Devagiri, "Assessment of above ground biomass and carbon pool in different vegetation types of south western part of Karnataka, India using spectral modeling," *Int. Soc. Trop. Ecol.*, vol. 54, no. 2, pp. 149–165, 2013.
- [54] N. I. Gasparri, M. G. Parmuchi, J. Bono, H. Karszenbaum, and C. L. Montenegro, "Assessing multi-temporal Landsat 7 ETM+ images for estimating above-ground biomass in subtropical dry forests of Argentina," *J. Arid Environ.*, vol. 74, no. 10, pp. 1262–1270, 2010.
- [55] European space agency (ESA), *Sentinel - 2 user handbook*. European space agency, 2015.
- [56] "Understanding Sentinel-2 Satellite Data – EOX." [online]. Available : <https://eox.at/2015/12/understanding-sentinel-2-satellite-data>. [Accessed : 30-Mar-2017].
- [57] J. Delegido, J. Verrelst, L. Alonso, and J. Moreno, "Evaluation of Sentinel-2 red-edge bands for empirical estimation of green LAI and chlorophyll content," *Sensors*, vol. 11, no. 7, pp. 7063–7081, 2011.
- [58] D. N. H. Horler, M. Dockray, and J. Barber, "The red edge of plant leaf reflectance," *Int. J. Remote Sens.*, 2007.
- [59] W. J. Frampton, J. Dash, G. Watmough, and E. J. Milton, "Evaluating the capabilities of Sentinel-2 for quantitative estimation of biophysical variables in vegetation," *ISPRS J. Photogramm. Remote Sens.*, vol. 82, pp. 83–92, 2013.
- [60] "Sentinel 2 EO Products | Sentinel." [Online]. Available: <http://www.sentinel-hub.com/apps/wms/wms-parameters/EoProducts>. [Accessed: 27-Mar-2017].
- [61] J. Delegido, J. Verrelst, L. Alonso, and J. Moreno, "Evaluation of Sentinel-2 red-edge bands for empirical estimation of green LAI and chlorophyll content," *Sensors*, vol. 11, no. 7, pp. 7063–7081, 2011.
- [62] Pemerintah Kabupaten Gunung Kidul, "BAB 2. Gambaran Umum Kabupaten Gunung Kidul." , Gunung Kidul, 2010.
- [63] "Pembangunan Kehutanan DIY - Jogja Masa Depan | Bappeda daerah Istimewa jogjakarta." [Online]. Available: http://bappeda.jogjapro.go.id/jogja_masa_depan/detail/Pembangunan-Kehutanan-DIY. [Accessed: 11-Jun-2017].
- [64] Arupa (Aliansi relawan penyelamat alam), *Menghitung cadangan karbon di hutan rakyat*. Jogjakarta: Arupa, 2014.
- [65] J. M. Chen, "Evaluation of Vegetation Indices and a Modified Simple Ratio for Boreal Applications," *Can. J. Remote Sens.*, vol. 22, no. 3, pp. 229–242, 1996.
- [66] T. Dong, J. Meng, J. Shang, J. Liu, and B. Wu, "Evaluation of Chlorophyll-Related Vegetation Indices Using Simulated Sentinel-2 Data for Estimation of Crop Fraction of Absorbed Photosynthetically Active Radiation," *IEEE J. Sel. Top. Appl. Earth Obs. Remote Sens.*, vol. 8, no. 8, pp. 4049–4059, 2015.

- [67] A. Minchella, "Sentinel-1 single image processing." Catapult satellite applications, 2016.
- [68] D. Small, "Flattening Gamma: Radiometric Terrain Correction for SAR Imagery," *IEEE Trans. Geosci. Remote Sens.*, vol. 49, no. 8, pp. 3081–3093, 2011.
- [69] A. Minchella, "Sentinel - 1 Overview." Catapult satellite applications, 2016.
- [70] Exelis, *Exploring ENVI*. Boulder, Colorado: Exelis VIS, 2015.
- [71] M. R. Chernick and R. H. Friis, *Introductory Biostatistics for the Health Sciences*. Hoboken, NJ, USA: John Wiley & Sons, Inc., 2003.
- [72] L. H. Kahane, *Regression Basics*, 2nd ed. Thousand Oaks : SAGE Publications, Inc., 2008.
- [73] J. T. Curtis and R. P. McIntosh, "The Interrelations of Certain Analytic and Synthetic Phytosociological Characters," *Ecology*, vol. 31, no. 3, pp. 434–455, 1950.
- [74] M. L. Imhoff, "Radar backscatter/biomass saturation: observations and implications for global biomass assessment," pp. 43–45, 1993.
- [75] Y. Rauste, T. Hame, J. Pullianen, K. Heiska, and M. hallikanen, "Radar-based forest biomass estimation," *Int. J. Remote Sens.*, vol. 15, no. 14, pp. 2797–2808, 1994.
- [76] R. A. Crabbe and D. W. Lamb, "Estimating biophysical variables of pasture cover using sentinel-1 data," *Zenodo*, 2017.
- [77] T. Le Toan *et al.*, "The BIOMASS mission: Mapping global forest biomass to better understand the terrestrial carbon cycle," *Remote Sens. Environ.*, vol. 115, no. 11, pp. 2850–2860, 2011.
- [78] S. Baig *et al.*, "Above Ground Biomass Estimation of Dalbergia sissoo Forest Plantation from Dual-Polarized ALOS-2 PALSAR Data," *Can. J. Remote Sens.*, vol. 43, no. 3, pp. 297–308, 2017.
- [79] G. Joseph, *Fundamentals of remote sensing*, Second. India: Universities pres, 2005.
- [80] S. Bousbih , "Potential of Sentinel-1 Radar Data for the Assessment of Soil and Cereal Cover Parameters," *Sensors*, vol. 17, no. 11, 2017.
- [81] A. Wijaya, S. Kusnadi, R. Gloaguen, and H. Heilmeyer, "Improved strategy for estimating stem volume and forest biomass using moderate resolution remote sensing data and GIS," *J. For. Res.*, vol. 21, no. 1, pp. 1–12, 2010.
- [82] R. Pu and J. Cheng, "Mapping forest leaf area index using reflectance and textural information derived from WorldView-2 imagery in a mixed natural forest area in Florida, US," *Int. J. Appl. Earth Obs. Geoinformation*, vol. 42, pp. 11–23, 2015.
- [83] C. Gómez, M. A. Wulder, F. Montes, and J. A. Delgado, "Forest structural diversity characterization in Mediterranean pines of central Spain with QuickBird-2 imagery and canonical correlation analysis," *Can. J. Remote Sens.*, vol. 37, no. 6, pp. 628–642, 2012.
- [84] P. Dusseux, L. Hubert-Moy, T. Corpetti, and F. Vertès, "Evaluation of SPOT imagery for the estimation of grassland biomass," *Int. J. Appl. Earth Obs. Geoinformation*, vol. 38, no. Supplement C, pp. 72–77, 2015.
- [85] B. Matsushita, W. Yang, J. Chen, Y. Onda, and G. Qiu, "Sensitivity of the Enhanced Vegetation Index (EVI) and Normalized Difference Vegetation Index (NDVI) to Topographic Effects: A Case Study in High-density Cypress Forest," *Sensors*, vol. 7, no. 11, pp. 2636–2651, 2007.

- [86] E. L. Garrouette, A. J. Hansen, and R. L. Lawrence, "Using NDVI and EVI to Map Spatiotemporal Variation in the Biomass and Quality of Forage for Migratory Elk in the Greater Yellowstone Ecosystem," *Remote Sens.*, vol. 8, no. 5, p. 404, 2016.
- [87] N. R. A. Jachowski, M. S. Y. Quak, D. A. Friess, D. Duangnamon, E. L. Webb, and A. D. Ziegler, "Mangrove biomass estimation in Southwest Thailand using machine learning," *Appl. Geogr.*, vol. 45, pp. 311–321, 2013.
- [88] K. C. Thumaty, R. Fararoda, S. Middinti, R. Gopalakrishnan, C. S. Jha, and V. K. Dadhwal, "Estimation of Above Ground Biomass for Central Indian Deciduous Forests Using ALOS PALSAR L-Band Data," *J. Indian Soc. Remote Sens.*, vol. 44, no. 1, pp. 31–39, 2016.
- [89] Z. Shao and L. Zhang, "Estimating Forest Aboveground Biomass by Combining Optical and SAR Data: A Case Study in Genhe, Inner Mongolia, China," *Sensors*, vol. 16, no. 6, 2016.
- [90] R. H. Purwanto, R. Rohman, A. Maryudi, T. Yuwono, D. B. Permadi, and M. Sanjaya, "Potensi Biomasa dan Simpanan Karbon Jenis-jenis Tanaman Berkayu di Hutan Rakyat Desa Nglanggeran, Gunungkidul, Daerah Istimewa Yogyakarta," *J. Ilmu Kehutan.*, vol. 6, no. 2, pp. 128–141, 2015.
- [91] S. Aminuddin, "Kajian potensi cadangan karbon pada pengusaha hutan rakyat (studi kasus : hutan rakyat Desa Dengok,kecamatan Playen,Kabupaten Gunung Kidul)," Institut pertanian Bogor, Bogor, 2008.
- [92] Arupa, *Proyeksi cadangan karbon hutan rakyat*. Jogjakarta: Biro penerbit arupa, 2014.

APPENDIX

Appendix 1 : data for AGB analysis

Table A : Summary of AGB based on the plots

| Plot Id | Total of trees | Mean DBH (cm) | Mean Height (m) | Plot coordinat (UTM) | | AGB (ton/ha) |
|---------|----------------|---------------|-----------------|----------------------|---------|--------------|
| | | | | x | y | |
| 1 | 18 | 13.69 | 8.37 | 441447 | 9110726 | 21 |
| 2 | 48 | 13.34 | 11.41 | 441321 | 9111438 | 98 |
| 3 | 37 | 15.33 | 13.1 | 441610 | 9110478 | 75 |
| 4 | 28 | 14.44 | 9.81 | 441612 | 9110650 | 64 |
| 5 | 25 | 17.11 | 9.42 | 441048 | 9111315 | 65 |
| 6 | 51 | 12.95 | 11.48 | 440987 | 9111407 | 175 |
| 7 | 34 | 15.54 | 12.73 | 440446 | 9111032 | 92 |
| 8 | 26 | 15.62 | 11.69 | 440766 | 9111539 | 69 |
| 9 | 23 | 12.39 | 9.2 | 440509 | 9111505 | 25 |
| 10 | 22 | 14.98 | 10.52 | 441822 | 9111808 | 69 |
| 11 | 24 | 12.08 | 10.68 | 441068 | 9112366 | 42 |
| 12 | 36 | 14.29 | 10.89 | 442113 | 9111812 | 63 |
| 13 | 34 | 15.56 | 13.86 | 440682 | 9110215 | 95 |
| 14 | 84 | 16.16 | 15.57 | 441611 | 9111807 | 84 |
| 15 | 24 | 15.15 | 14.47 | 441496 | 9110425 | 101 |
| 16 | 34 | 13.63 | 14.08 | 441937 | 9110205 | 71 |
| 17 | 30 | 10.92 | 12.82 | 441047 | 9112577 | 67 |
| 18 | 34 | 14.07 | 11.46 | 443536 | 9111828 | 125 |
| 19 | 51 | 13.38 | 10.29 | 443659 | 9111407 | 175 |
| 20 | 29 | 15.9 | 12.78 | 443747 | 9112222 | 101 |
| 21 | 40 | 14.68 | 11.87 | 443867 | 9111848 | 137 |
| 22 | 44 | 14.93 | 12.85 | 443478 | 9112123 | 226 |
| 23 | 38 | 12.24 | 10.92 | 443694 | 9112805 | 48 |
| 24 | 26 | 15.32 | 11.43 | 443547 | 9112882 | 58 |
| 25 | 51 | 12.76 | 11.04 | 443399 | 9111751 | 158 |
| 26 | 23 | 11.92 | 9.55 | 444524 | 9112758 | 32 |
| 27 | 30 | 13.45 | 10.3 | 444129 | 9112382 | 32 |
| 28 | 31 | 16.75 | 13.4 | 441993 | 9111789 | 106 |
| 29 | 42 | 10.97 | 11.87 | 441745 | 9109996 | 62 |
| 30 | 28 | 12.73 | 10 | 442617 | 9112183 | 90 |

| | | | | | | |
|----|----|-------|-------|--------|---------|-----|
| 31 | 29 | 15.24 | 13.78 | 440118 | 9111013 | 86 |
| 32 | 44 | 12.5 | 10.95 | 442691 | 9111828 | 125 |
| 33 | 41 | 13.17 | 14.24 | 441434 | 9111322 | 82 |
| 34 | 33 | 16.25 | 13.21 | 441691 | 9111138 | 96 |
| 35 | 25 | 16.39 | 15.69 | 441211 | 9111251 | 74 |
| 36 | 39 | 13.72 | 10.63 | 440587 | 9110836 | 93 |
| 37 | 38 | 12.58 | 12.04 | 441248 | 9110698 | 82 |
| 38 | 16 | 6.71 | 14.82 | 441035 | 9112470 | 97 |
| 39 | 33 | 13.31 | 10.95 | 440691 | 9110360 | 56 |
| 40 | 35 | 13.18 | 13.86 | 440957 | 9110833 | 76 |
| 41 | 29 | 11.3 | 11.27 | 441371 | 9110394 | 43 |
| 42 | 38 | 12.36 | 11.61 | 443713 | 9112136 | 61 |
| 43 | 27 | 17.17 | 17.78 | 440687 | 9111232 | 80 |
| 44 | 21 | 16.17 | 10.64 | 441535 | 9111184 | 56 |
| 45 | 24 | 16.93 | 13.28 | 441529 | 9110901 | 75 |

Table B : data for correlation between AGB and Vegetation indices

| Plot ID | AGB (ton/ha) | ND45 | NDVI | SR | IRECI | NDI75 | EVI |
|---------|--------------|------|------|-------|-------|-------|------|
| 1 | 21 | 0.59 | 0.84 | 11.60 | 0.61 | 0.43 | 0.48 |
| 2 | 98 | 0.70 | 0.92 | 24.64 | 1.10 | 0.57 | 0.57 |
| 3 | 75 | 0.66 | 0.89 | 17.36 | 0.80 | 0.50 | 0.51 |
| 4 | 64 | 0.59 | 0.87 | 14.43 | 1.02 | 0.51 | 0.59 |
| 5 | 65 | 0.57 | 0.84 | 11.71 | 0.91 | 0.48 | 0.59 |
| 6 | 175 | 0.79 | 0.96 | 44.78 | 1.27 | 0.62 | 0.56 |
| 7 | 92 | 0.64 | 0.89 | 17.03 | 1.16 | 0.52 | 0.66 |
| 8 | 69 | 0.63 | 0.88 | 15.52 | 0.98 | 0.50 | 0.61 |
| 9 | 25 | 0.58 | 0.86 | 13.26 | 1.01 | 0.50 | 0.61 |
| 10 | 69 | 0.65 | 0.89 | 16.89 | 0.91 | 0.50 | 0.56 |
| 11 | 42 | 0.54 | 0.79 | 8.32 | 0.46 | 0.36 | 0.42 |
| 12 | 63 | 0.64 | 0.87 | 14.37 | 0.91 | 0.47 | 0.60 |
| 13 | 95 | 0.66 | 0.89 | 16.42 | 0.94 | 0.49 | 0.60 |
| 14 | 84 | 0.69 | 0.91 | 20.71 | 0.85 | 0.53 | 0.50 |
| 15 | 101 | 0.65 | 0.90 | 18.94 | 1.02 | 0.54 | 0.57 |
| 16 | 71 | 0.62 | 0.88 | 15.14 | 1.08 | 0.50 | 0.64 |
| 17 | 67 | 0.63 | 0.90 | 19.44 | 1.07 | 0.57 | 0.56 |
| 18 | 125 | 0.69 | 0.91 | 20.69 | 1.16 | 0.53 | 0.65 |
| 19 | 175 | 0.75 | 0.93 | 26.12 | 1.15 | 0.53 | 0.65 |
| 20 | 101 | 0.69 | 0.91 | 21.37 | 0.94 | 0.54 | 0.55 |
| 21 | 137 | 0.71 | 0.92 | 23.51 | 1.18 | 0.54 | 0.63 |
| 22 | 226 | 0.84 | 0.96 | 51.91 | 1.21 | 0.57 | 0.62 |
| 23 | 48 | 0.57 | 0.87 | 14.58 | 1.12 | 0.54 | 0.62 |
| 24 | 58 | 0.57 | 0.83 | 11.04 | 0.79 | 0.46 | 0.55 |
| 25 | 158 | 0.71 | 0.92 | 25.53 | 1.24 | 0.57 | 0.62 |
| 26 | 32 | 0.55 | 0.80 | 9.19 | 0.66 | 0.41 | 0.52 |
| 27 | 32 | 0.58 | 0.85 | 12.11 | 0.69 | 0.47 | 0.49 |
| 28 | 106 | 0.72 | 0.91 | 20.33 | 0.85 | 0.48 | 0.59 |
| 29 | 62 | 0.63 | 0.90 | 18.30 | 0.84 | 0.55 | 0.47 |
| 30 | 90 | 0.75 | 0.94 | 34.88 | 1.09 | 0.59 | 0.54 |

Table C : data for correlation between AGB and spectral reflectance

| No | AGB (ton/ha) | B3 | B4 | B5 | B6 | B7 | B8 |
|-----------|---------------------|-----------|-----------|-----------|-----------|-----------|-----------|
| 1 | 21 | 0.047 | 0.023 | 0.09 | 0.23 | 0.27 | 0.29 |
| 2 | 98 | 0.035 | 0.013 | 0.07 | 0.27 | 0.32 | 0.32 |
| 3 | 75 | 0.034 | 0.016 | 0.08 | 0.24 | 0.28 | 0.26 |
| 4 | 64 | 0.050 | 0.024 | 0.09 | 0.29 | 0.35 | 0.34 |
| 5 | 65 | 0.059 | 0.030 | 0.11 | 0.31 | 0.35 | 0.37 |
| 6 | 175 | 0.023 | 0.007 | 0.06 | 0.24 | 0.30 | 0.34 |
| 7 | 92 | 0.054 | 0.023 | 0.11 | 0.33 | 0.39 | 0.37 |
| 8 | 69 | 0.054 | 0.023 | 0.10 | 0.30 | 0.35 | 0.37 |
| 9 | 25 | 0.059 | 0.028 | 0.10 | 0.31 | 0.37 | 0.38 |
| 10 | 69 | 0.044 | 0.019 | 0.09 | 0.27 | 0.32 | 0.34 |
| 11 | 42 | 0.053 | 0.029 | 0.10 | 0.21 | 0.24 | 0.28 |
| 12 | 63 | 0.053 | 0.024 | 0.11 | 0.30 | 0.35 | 0.37 |
| 13 | 95 | 0.055 | 0.021 | 0.10 | 0.30 | 0.35 | 0.36 |
| 14 | 84 | 0.029 | 0.013 | 0.07 | 0.23 | 0.28 | 0.25 |
| 15 | 101 | 0.037 | 0.017 | 0.08 | 0.26 | 0.32 | 0.29 |
| 16 | 71 | 0.056 | 0.026 | 0.11 | 0.33 | 0.39 | 0.40 |
| 17 | 67 | 0.034 | 0.016 | 0.07 | 0.25 | 0.31 | 0.30 |
| 18 | 125 | 0.047 | 0.018 | 0.10 | 0.32 | 0.38 | 0.39 |
| 19 | 175 | 0.045 | 0.014 | 0.10 | 0.32 | 0.37 | 0.37 |
| 20 | 101 | 0.038 | 0.014 | 0.08 | 0.25 | 0.29 | 0.29 |
| 21 | 137 | 0.043 | 0.016 | 0.09 | 0.31 | 0.37 | 0.36 |
| 22 | 226 | 0.029 | 0.007 | 0.08 | 0.28 | 0.34 | 0.34 |
| 23 | 48 | 0.048 | 0.024 | 0.09 | 0.30 | 0.36 | 0.37 |
| 24 | 58 | 0.057 | 0.029 | 0.10 | 0.28 | 0.32 | 0.35 |
| 25 | 158 | 0.042 | 0.014 | 0.08 | 0.30 | 0.35 | 0.36 |
| 26 | 32 | 0.057 | 0.033 | 0.11 | 0.27 | 0.31 | 0.30 |
| 27 | 32 | 0.046 | 0.022 | 0.08 | 0.23 | 0.27 | 0.27 |
| 28 | 106 | 0.048 | 0.016 | 0.10 | 0.28 | 0.32 | 0.37 |
| 29 | 62 | 0.029 | 0.014 | 0.06 | 0.21 | 0.26 | 0.25 |
| 30 | 90 | 0.028 | 0.008 | 0.06 | 0.23 | 0.29 | 0.30 |

Table D : Data for correlation between AGB and Sentinel-1 backscatter

| Plot ID | AGB (ton/ha) | Gamma VH | Gamma VV |
|---------|--------------|----------|----------|
| 1 | 21 | -10.68 | -4.45 |
| 2 | 98 | -13.31 | -7.52 |
| 3 | 75 | -13.42 | -9.55 |
| 4 | 64 | -13.43 | -7.50 |
| 5 | 65 | -11.53 | -7.25 |
| 6 | 175 | -12.74 | -9.43 |
| 7 | 92 | -11.11 | -6.48 |
| 8 | 69 | -13.69 | -8.47 |
| 9 | 25 | -12.45 | -8.62 |
| 10 | 69 | -12.65 | -7.39 |
| 11 | 42 | -13.26 | -7.96 |
| 12 | 63 | -14.25 | -6.42 |
| 13 | 95 | -11.49 | -5.18 |
| 14 | 84 | -11.77 | -4.10 |
| 15 | 101 | -12.50 | -7.77 |
| 16 | 71 | -13.75 | -8.46 |
| 17 | 67 | -15.05 | -11.78 |
| 18 | 125 | -11.86 | -6.70 |
| 19 | 175 | -15.44 | -8.11 |
| 20 | 101 | -14.96 | -7.05 |
| 21 | 137 | -12.49 | -6.69 |
| 22 | 226 | -13.88 | -8.27 |
| 23 | 48 | -13.50 | -5.71 |
| 24 | 58 | -11.07 | -4.77 |
| 25 | 158 | -14.12 | -8.55 |
| 26 | 32 | -11.44 | -8.30 |
| 27 | 32 | -9.61 | -4.43 |
| 28 | 106 | -14.33 | -6.99 |
| 29 | 62 | -13.43 | -8.17 |
| 30 | 90 | -10.26 | -5.69 |

Table E : Data for AGB validation

| Plot Id | Observed AGB (ton/ha) | Predicted AGB (ton/ha) |
|----------------|------------------------------|-------------------------------|
| 31 | 86 | 120 |
| 32 | 125 | 175 |
| 33 | 82 | 123 |
| 34 | 96 | 112 |
| 35 | 74 | 103 |
| 36 | 93 | 118 |
| 37 | 82 | 94 |
| 38 | 97 | 125 |
| 39 | 56 | 56 |
| 40 | 76 | 114 |
| 41 | 43 | 72 |
| 42 | 61 | 73 |
| 43 | 80 | 68 |
| 44 | 56 | 37 |
| 45 | 75 | 72 |

Appendix 2 : Statistical analysis

Table F : Correlation analysis between AGB and vegetation indices

| | | Correlations | | | | | | |
|-------|---------------------|--------------|--------|--------|--------|--------|--------|--------|
| | | AGB | ND45 | SR | IRECI | nd75 | evi | NDVI |
| AGB | Pearson Correlation | 1 | ,893** | ,857** | ,700** | ,623** | ,486** | ,806** |
| | Sig. (2-tailed) | | ,000 | ,000 | ,000 | ,000 | ,006 | ,000 |
| | N | 30 | 30 | 30 | 30 | 30 | 30 | 30 |
| ND45 | Pearson Correlation | ,893** | 1 | ,573** | ,414* | ,752** | ,163 | ,576** |
| | Sig. (2-tailed) | ,000 | | ,001 | ,021 | ,000 | ,380 | ,001 |
| | N | 30 | 31 | 31 | 31 | 31 | 31 | 31 |
| SR | Pearson Correlation | ,857** | ,573** | 1 | ,675** | ,544** | ,328 | ,876** |
| | Sig. (2-tailed) | ,000 | ,001 | | ,000 | ,002 | ,072 | ,000 |
| | N | 30 | 31 | 31 | 31 | 31 | 31 | 31 |
| IRECI | Pearson Correlation | ,700** | ,414* | ,675** | 1 | ,677** | ,822** | ,805** |
| | Sig. (2-tailed) | ,000 | ,021 | ,000 | | ,000 | ,000 | ,000 |
| | N | 30 | 31 | 31 | 31 | 31 | 31 | 31 |
| nd75 | Pearson Correlation | ,623** | ,752** | ,544** | ,677** | 1 | ,273 | ,676** |
| | Sig. (2-tailed) | ,000 | ,000 | ,002 | ,000 | | ,137 | ,000 |
| | N | 30 | 31 | 31 | 31 | 31 | 31 | 31 |
| Evi | Pearson Correlation | ,486** | ,163 | ,328 | ,822** | ,273 | 1 | ,484** |
| | Sig. (2-tailed) | ,006 | ,380 | ,072 | ,000 | ,137 | | ,006 |
| | N | 30 | 31 | 31 | 31 | 31 | 31 | 31 |
| NDVI | Pearson Correlation | ,806** | ,576** | ,876** | ,805** | ,676** | ,484** | 1 |
| | Sig. (2-tailed) | ,000 | ,001 | ,000 | ,000 | ,000 | ,006 | |
| | N | 30 | 31 | 31 | 31 | 31 | 31 | 31 |

** . Correlation is significant at the 0.01 level (2-tailed).

* . Correlation is significant at the 0.05 level (2-tailed).

Table G : Correlation analysis between AGB and vegetation indices

| | | Correlations | | | | | | |
|-----|---------------------|--------------|---------|---------|--------|--------|--------|--------|
| | | AGB | B3 | B4 | B5 | B6 | B7 | B8 |
| AGB | Pearson Correlation | 1 | -,492** | -,727** | -,332 | ,199 | ,300 | ,241 |
| | Sig. (2-tailed) | | ,006 | ,000 | ,073 | ,291 | ,107 | ,200 |
| | N | 30 | 30 | 30 | 30 | 30 | 30 | 30 |
| B3 | Pearson Correlation | -,492** | 1 | ,998** | ,994** | ,420* | ,160 | ,408* |
| | Sig. (2-tailed) | ,006 | | ,000 | ,000 | ,019 | ,391 | ,023 |
| | N | 30 | 31 | 31 | 31 | 31 | 31 | 31 |
| B4 | Pearson Correlation | -,727** | ,998** | 1 | ,986** | ,378* | ,121 | ,366* |
| | Sig. (2-tailed) | ,000 | ,000 | | ,000 | ,036 | ,518 | ,043 |
| | N | 30 | 31 | 31 | 31 | 31 | 31 | 31 |
| B5 | Pearson Correlation | -,332 | ,994** | ,986** | 1 | ,485** | ,221 | ,462** |
| | Sig. (2-tailed) | ,073 | ,000 | ,000 | | ,006 | ,232 | ,009 |
| | N | 30 | 31 | 31 | 31 | 31 | 31 | 31 |
| B6 | Pearson Correlation | ,199 | ,420* | ,378* | ,485** | 1 | ,946** | ,910** |
| | Sig. (2-tailed) | ,291 | ,019 | ,036 | ,006 | | ,000 | ,000 |
| | N | 30 | 31 | 31 | 31 | 31 | 31 | 31 |
| B7 | Pearson Correlation | ,300 | ,160 | ,121 | ,221 | ,946** | 1 | ,876** |
| | Sig. (2-tailed) | ,107 | ,391 | ,518 | ,232 | ,000 | | ,000 |
| | N | 30 | 31 | 31 | 31 | 31 | 31 | 31 |
| B8 | Pearson Correlation | ,241 | ,408* | ,366* | ,462** | ,910** | ,876** | 1 |
| | Sig. (2-tailed) | ,200 | ,023 | ,043 | ,009 | ,000 | ,000 | |
| | N | 30 | 31 | 31 | 31 | 31 | 31 | 31 |

** . Correlation is significant at the 0.01 level (2-tailed).

* . Correlation is significant at the 0.05 level (2-tailed).

Table H . Correlation between AGB and SAR backscatter

| | | Correlations | | |
|----------|---------------------|--------------|----------|----------|
| | | AGB | Gamma VH | Gamma VV |
| AGB | Pearson Correlation | 1 | -,369* | -,238 |
| | Sig. (2-tailed) | | ,045 | ,206 |
| | N | 30 | 30 | 30 |
| Gamma VH | Pearson Correlation | -,369* | 1 | ,779** |
| | Sig. (2-tailed) | ,045 | | ,000 |
| | N | 30 | 31 | 31 |
| Gamma VV | Pearson Correlation | -,238 | ,779** | 1 |
| | Sig. (2-tailed) | ,206 | ,000 | |
| | N | 30 | 31 | 31 |

*. Correlation is significant at the 0.05 level (2-tailed).

**. Correlation is significant at the 0.01 level (2-tailed).

Table I Statistical summary of AGB model

| Model Summary | | | | | | | | |
|---------------------------|-------------------|-----------------------------|-------------------|----------------------------|--------|-------------------|-------------------------|-------|
| Model | R | R Square | Adjusted R Square | Std. Error of the Estimate | | | | |
| 1 | ,911 ^b | .831 | .818 | 20.499 | | | | |
| | | | | | | | | |
| ANOVA ^a | | | | | | | | |
| Model | | Sum of Squares | df | Mean Square | F | Sig. | | |
| 1 | Regression | 55719.595 | 2 | 27859.797 | 66.299 | ,000 ^c | | |
| | Residual | 11345.872 | 27 | 420.217 | | | | |
| | Total | 67065.467 | 29 | | | | | |
| | | | | | | | | |
| Coefficients ^a | | | | | | | | |
| Model | | Unstandardized Coefficients | | Standardized Coefficients | t | Sig. | Collinearity Statistics | |
| | | B | Std. Error | Beta | | | Tolerance | VIF |
| 1 | (Constant) | -353.661 | 42.930 | | -8.238 | .000 | | |
| | ND45 | 537.391 | 55.169 | .824 | 9.741 | .000 | .876 | 1.141 |
| | evi | 158.423 | 68.279 | .196 | 2.320 | .028 | .876 | 1.141 |

Table J. Statistical summary AGB map validation

| Model Summary | | | | | | |
|---------------------------|-------------------|-----------------------------|-------------------|----------------------------|--------|-------------------|
| Model | R | R Square | Adjusted R Square | Std. Error of the Estimate | | |
| 1 | ,864 ^a | .746 | .726 | 18.1971054 | | |
| | | | | | | |
| Anova | | | | | | |
| Model | | Sum of Squares | df | Mean Square | F | Sig. |
| 1 | Regression | 12644.105 | 1 | 12644.105 | 38.184 | ,000 ^b |
| | Residual | 4304.750 | 13 | 331.135 | | |
| | Total | 16948.855 | 14 | | | |
| | | | | | | |
| Coefficients ^a | | | | | | |
| Model | | Unstandardized Coefficients | | Standardized Coefficients | t | Sig. |
| | | B | Std. Error | Beta | | |
| 1 | (Constant) | 29.850 | 19.533 | | -1.004 | .334 |
| | Predicted | 0.50 | .241 | .864 | 6.179 | .000 |

Appendix 3

Table K. Accuracy assesment of landcover classification

| No | Item | Item | | |
|----|--------------|-----------|------------|------------|
| | | Forest | Non forest | Total |
| 1 | Forest | 90 | 5 | 95 |
| 2 | Non forest | 5 | 60 | 65 |
| | Total | 95 | 65 | 160 |

Classification accuracy for forest :

1. User's accuracy : $\frac{90}{95} = 0.95$

2. Producer's accuracy : $\frac{90}{95} = 0.95$

3. Overall accuracy : $\frac{(90+60)}{160} = 0.94$

Appendix 4
Documentation



Documentation 1. Establishing of sample plots



Documentation 2. Marking of trees within the plot



Documentation 3. Measuring circumference of tree



Documentation 4. Measuring height of tree



Documentation 5. Recording of field data



Documentation 6. Team survey

VITAE

Name Askar
Student ID 5910920038

Educational Attainment

| Degree | Name of Institution | Year of Graduation |
|---------------------|----------------------------|---------------------------|
| Bachelor of Science | Universitas Gadjah Mada | 2007 |

Scholarship Awards during Enrolment

1. Thailand's Education Hub for Southern Region of ASEAN Countries, Prince of Songkla University, 2017-2019 (Grant No: TEH-AC 013/2016).
2. Graduate School Research Funding For Thesis, Prince of Songkla University, for Master Student, 2017.

Work – Position and Address

Mapping Staff at Social Forestry and Environmental Partnership Agency of Sulawesi, Ministry of Environmental and Forestry of Indonesia. Address : Bili – bili, Gowa regency, South Sulawesi Province, Indonesia.

List of Publication

1. Askar, Narissara Nuthammachot, Tri Sayektiningsih and Hermudananto (2018). Assessing Land Cover Changes and CO₂ Emissions in Tropical Forest in 1998-2016: Study Case Of The Sungai Wain Protection Forest. Polish Journal of Environmental Studies (ISI, Q4, IF = 1.1, Accepted: 04/09/2018).
2. Askar, Narissara Nuthammachot, Worradorn Phairuang, Pramaditya Wicaksono, Tri Sayektiningsih. Estimation above ground biomass on private forest using Sentinel-2 imagery. Journal of Sensors (ISI, Q2, IF = 2.0, Accepted :30 /9/2018).